Monthly Notices
of the
ROYAL ASTRONOMICAL SOCIETY

Mon. Not. R. Astron. Soc. **413,** 1036–1053 (2011) doi:10.1111/j.1365-2966.2011.18195.x

The stellar populations of early-type galaxies – II. The effects of environment and mass

Craig D. Harrison,[1,2⋆] Matthew Colless,[3] Harald Kuntschner,[4] Warrick J. Couch,[5] Roberto De Propris[2] and Michael B. Pracy[5]

[1]*Research School of Astronomy & Astrophysics, Australian National University, Weston Creek, ACT 2611, Australia*
[2]*Cerro Tololo Inter-American Observatory, Casilla 603, La Serena, Chile*
[3]*Anglo-Australian Observatory, PO Box 296, Epping, NSW 2111, Australia*
[4]*Space Telescope European Coordinating Facility, European Southern Observatory, Karl-Schwarzschild-Str, 85748 Garching, Germany*
[5]*Centre for Astrophysics & Supercomputing, Swinburne University of Technology, PO Box 218, Hawthorn, VIC 3122, Australia*

Accepted 2010 December 10. Received 2010 November 22; in original form 2010 April 28

ABSTRACT

The degree of influence that the environment and mass have on the stellar populations of early-type galaxies is uncertain. In this paper, we present the results of a spectroscopic analysis of the stellar populations of early-type galaxies aimed at addressing this question. The sample of galaxies is drawn from four clusters, with $\langle z \rangle = 0.04$, and their surrounding structure extending to $\sim 10 R_{\rm vir}$. We find that the distributions of the absorption-line strengths and the stellar population parameters, age, metallicity and α-element abundance ratio, do not differ significantly between the clusters and their outskirts, but the tight correlations found between these quantities and the velocity dispersion within the clusters are weaker in their outskirts. All three stellar population parameters of cluster galaxies are positively correlated with the velocity dispersion. Galaxies in clusters form a homogeneous class of objects that have similar distributions of line-strengths and stellar population parameters, and follow similar scaling relations, regardless of the cluster richness or morphology. We estimate the intrinsic scatter of the Gaussian distribution of metallicities to be 0.3 dex, while that of the α-element abundance ratio is 0.07 dex. The e-folding time of the exponential distribution of galaxy ages is estimated to be 900 Myr. The intrinsic scatters of the metallicity and α-element abundance ratio distributions can almost entirely be accounted for by the correlations with the velocity dispersion and the intrinsic scatter about these relations. This implies that the galaxy mass plays a major role in determining its stellar population.

Key words: galaxies: clusters: general – galaxies: elliptical and lenticular, cD – galaxies: formation – galaxies: stellar content.

1 INTRODUCTION

The classical model of the galaxy formation, the monolithic collapse model (Eggen, Lynden-Bell & Sandage 1962; Larson 1974, 1975; Tinsley & Gunn 1976; Arimoto & Yoshii 1987; Bressan, Chiosi & Fagotto 1994), proposes that galaxies form in a single massive collapse at high redshift and that the subsequent evolution is purely passive. This model has been overtaken by the current dominant model of the galaxy formation, the hierarchical merging model (Toomre 1977; Searle & Zinn 1978; White & Rees 1978), which proposes that galaxies are built up through mergers: small objects form first and undergo a series of mergers that build up more massive objects. A third scenario, the revised monolithic collapse model (e.g. Merlin & Chiosi 2006), proposes that galaxies form in a number of rapid mergers at high redshift before evolving passively.

Galaxy clusters originate from the most-extreme density fluctuations, where the galaxy formation and evolution is expected to proceed at an accelerated rate. Moreover, the stellar populations of galaxies moving into a cluster environment are expected to be modified via interactions with other galaxies and the dense intracluster medium. These interactions can be roughly divided into two broad classes: local processes including mergers (Toomre 1977) and tidal interactions (Mastropietro et al. 2005); and global processes including the ram pressure stripping (Gunn & Gott 1972), interactions with the cluster tidal field (Bekki 1999), harassment (Moore et al. 1999) and strangulation (Larson, Tinsley & Caldwell 1980). Local processes are more efficient in galaxy groups where relative velocities are lower, while global processes are more efficient in clusters where the frequency of interaction is higher.

⋆E-mail: charrison@ctio.noao.edu

Correlations are therefore expected between galaxy observables and the environment (Kauffmann 1996; Kauffmann & Charlot 1998), and have been found for the galaxy morphology (Davis & Geller 1976; Dressler 1980; Postman & Geller 1984; Balogh et al. 1998), colour (Blanton et al. 2005), Sérsic index (Hashimoto & Oemler 1999; Blanton et al. 2005), star formation rate (Lewis et al. 2002; Gómez et al. 2003; Boselli & Gavazzi 2006) and spectral type (Norberg et al. 2002). However, in a comprehensive study of the dependence of galaxy observables on the environment within the SDSS, Blanton et al. (2005) suggest that the structural properties of galaxies are less dependent on the environment than on their masses and star formation histories.

To add to this debate, Fundamental Plane studies have found no differences between field galaxies more massive than $2 \times 10^{11}\,\mathrm{M}_{\odot}$ and their counterparts in clusters at the same redshift (Treu et al. 1999, 2001; van Dokkum et al. 2001), while less-massive galaxies were found to be younger in the field (Treu et al. 2002; van Dokkum & Stanford 2003; van der Wel et al. 2004, 2005; Treu et al. 2005a,b). This might imply that the star formation in field galaxies occurs first in the most-massive galaxies and then progressively in less-massive galaxies, and that the mass rather than the environment governs the overall growth.

The Lick system of absorption-line indices (Burstein et al. 1984; Faber et al. 1985; Burstein, Faber & Gonzalez 1986; Gorgas et al. 1993; Worthey et al. 1994; Trager et al. 1998) and associated models (e.g. Worthey 1994; Thomas, Maraston & Bender 2003; Thomas, Maraston & Korn 2004), from which the stellar population parameters (SPPs), age, metallicity ([Z/H]) and α-element abundance ratio ([α/Fe]), can be estimated, provide an excellent method with which to study the role of the mass and environment in determining galaxy properties.

The line-strengths of early-type galaxies are found to be correlated with the velocity dispersion (σ). Lick indices that are more sensitive to [Z/H] effects, for example, Mg*b*, are positively correlated (Burstein et al. 1988; Bender, Burstein & Faber 1993; Ziegler & Bender 1997; Colless et al. 1999; Kuntschner 2000), while those indices more sensitive to age effects, for example, Hβ, are negatively correlated (Fisher, Franx & Illingworth 1995, 1996; Jørgensen 1997, 1999a; Kuntschner 2000; Bernardi et al. 2003; Caldwell, Rose & Concannon 2003). Although both elements are sensitive to [Z/H], the slope of the correlation between Mg and the velocity dispersion is found to be much steeper than that of Fe (Worthey, Faber & Gonzalez 1992; Fisher et al. 1995; Greggio 1997; Jørgensen 1999a; Kuntschner 2000; Terlevich & Forbes 2002).

These index–σ correlations suggest that the SPPs should also be correlated with the velocity dispersion. Given the difference in the slopes of the Mg–σ and Fe–σ relations, a correlation between [α/Fe] and the velocity dispersion was expected and has been confirmed (Trager et al. 2000a; Proctor & Sansom 2002; Thomas, Maraston & Bender 2002; Mehlert et al. 2003; Thomas et al. 2005). If the α-element enhancement is due to the time-scale of the star formation and the velocity dispersion is a proxy for the mass, then this correlation indicates that more massive galaxies form their stars on shorter time-scales than less-massive galaxies.

[Z/H] of a galaxy is also found to correlate with the velocity dispersion (Greggio 1997; Thomas et al. 2005), with massive galaxies being more metal rich. Such a relation is a natural consequence of galactic wind models (e.g. Arimoto & Yoshii 1987), which show that larger gravitational potential of massive galaxies allows them to better retain their heavy elements.

Whether a correlation exists between the age and velocity dispersion is still uncertain. Early studies found no significant correlation (Trager et al. 2000a; Kuntschner et al. 2001; Terlevich & Forbes 2002), but recent studies have detected a weak but significant correlation having large scatter (Proctor & Sansom 2002; Proctor et al. 2004a; Proctor, Forbes & Beasley 2004b; Thomas et al. 2005), with more massive galaxies being older. This trend which would indicate that more massive galaxies formed their stellar content earlier is in agreement with the concept of the downsizing (Cowie et al. 1996) and the latest semianalytic models of the galaxy formation (e.g. De Lucia et al. 2006).

Early-type galaxies in low-density environments exhibit small differences compared to those in clusters: at a given luminosity, the early-type galaxies in low-density regions are ∼1–3 Gyr younger and 0.1–0.2 dex more metal rich than those in clusters (Trager et al. 2000a; Poggianti et al. 2001; Kuntschner et al. 2002; Terlevich & Forbes 2002; Caldwell et al. 2003; Proctor et al. 2004a; Thomas et al. 2005; Sánchez-Blázquez et al. 2006). In conflict with the above results, Gallazzi et al. (2006), using a large sample of early-type galaxies from the SDSS, found evidence that galaxies in low-density environments were less metal rich than those in high-density environments. Intriguingly, there appears to be no environmental dependence of [α/Fe] (Kuntschner et al. 2002; Thomas et al. 2005), indicating that the star formation in galaxies of a given mass occurs on the same time-scale whether they are located in high-density or low-density environments.

While it appears that the stellar populations of galaxies change from low-density environments to high-density environments, the density threshold at which this change occurs is uncertain. Studies of the star formation rate of galaxies in and around clusters (Lewis et al. 2002; Gómez et al. 2003) find an increase in the star formation rate with increasing distance from the cluster centre, converging to the mean field rate at distances greater than $\sim 3R_{\mathrm{vir}}$. The critical projected density at which suppression of the star formation begins is uncertain, but the environmental influences on galaxy properties are believed not to be restricted to cluster cores, being effective in all groups where the density exceeds the critical value. The observed low rates of the star formation well beyond the virialized cluster rule out physical processes associated with extreme environments (such as the ram pressure stripping of the disc gas) being completely responsible for the variations in galaxy properties with the environment.

This paper is the second in a series of papers aimed at studying the effects of the environment and mass on the stellar populations of early-type galaxies. The first paper described our sample selection, observations, data reductions and method of measuring line-strengths and estimating SPPs within the framework of the Lick system. In this paper, we present the results of this study utilizing data from four clusters and their surrounds. The data extend to $\sim 10R_{\mathrm{vir}}$, allowing us to probe the in-fall regions of the clusters, which to date have been poorly studied. The layout of the remainder of the paper is as follows. Section 2 briefly describes the sample, observations and reductions, measurement of Lick indices and SPP estimation. Analysis of the absorption-line strengths is detailed in Section 3 and that of the distributions of the SPPs is detailed in Section 4. The correlations between the SPPs and velocity dispersion are discussed in Section 5, while the contribution from these correlations to the intrinsic scatter in the parameter distributions is investigated in Section 6. We discuss the results of this study in Section 7 and present a summary of this work in Section 8.

A Hubble parameter $H_0 = 70\,\mathrm{km\,s^{-1}\,Mpc^{-1}}$, matter density parameter $\Omega_{\mathrm{M}} = 0.3$ and dark energy density parameter $\Omega_{\Lambda} = 0.7$ are adopted throughout this work.

2 FROM OBSERVATIONS TO STELLAR POPULATION PARAMETERS

Details of the observations, data reductions, measurement of Lick indices and estimation of the corresponding SPPs are given in Harrison et al. (2010, hereinafter referred to as Paper I). Therefore, only brief descriptions will be given here.

Observations of galaxies from four clusters (A930, A1139, A3558 and Coma) of varying richness and morphology were made with the 2dF during the nights of 2002 April 19–21. Observations of galaxies from the same four clusters and the structures around them were made with the 6dF during the nights of 2003 March 6–8. The 6dF sample contained some galaxies in common with the 2dF sample, but mostly consisted of galaxies in the outer regions of each cluster. In two of the fields (A1139 and A930), the observations were offset from the cluster centre, allowing galaxies with clustercentric distances of up to $\sim 19\,h_{70}^{-1}$ Mpc to be studied. The set-up of the two instruments can be found in Paper I.

A brief discussion of the way galaxies were classified as early types or not is warranted here. This was done spectroscopically with galaxies that showed signs of the Hα (EW < -3.8 Å) or [O III] λ5007 Å (EW < -0.4 Å) emission being classified as star forming. We chose to classify a galaxy by its spectrum because comparisons to SSP models are (almost) meaningless in galaxies with significant emission. The in-fill of the Hβ absorption feature by the nebular emission results in weaker Hβ line-strengths and incorrectly older ages. Some methods used to correct for this nebular in-fill (e.g. González 1993; Trager et al. 2000a,b) have proved unsatisfactory, while others (Sarzi et al. 2006) can only correct for relatively weak emission. For these reasons we eliminated all galaxies with signs of emission from our sample of early types. It must be noted that, in doing so, it is possible that we exclude from our stellar population analysis early-type galaxies that have had star formation triggered by the cluster environment.

Other methods of classifying galaxies are not problem-free. Classifying by the morphology is highly subjective and samples selected by colour–magnitude cuts still contain contamination by galaxies that would have been morphologically classified as late types. More importantly, these methods do not eliminate all emission-line galaxies; up to 30 per cent of red-sequence galaxies can show signs of the low-ionization nuclear emission-line region emission (Graves et al. 2007) and so the interpretation of a stellar population analysis for these galaxies would be difficult.

However, the absence of emission lines does not guarantee that a galaxy has not had significant star formation in its recent past and so it is possible that our sample of early types contains a small number of post-starburst galaxies. The intrinsic scatters in the line-strength–σ (Section 3.1) and SPP–σ relations (Section 5.1) are comparable to published results implying that if our sample contains recently star-forming galaxies, then it is in no greater number than previous samples.

The basic reduction steps, such as bias subtraction, spectrum extraction, flat-fielding, wavelength calibration, fibre throughput determination and correction, and sky subtraction, were performed with the purpose-built data-reduction packages 2DFDR (Colless et al. 2001) and 6DFDR (Jones et al. 2004). Redshifts were measured using the program RUNZ (Colless et al. 2001), while the IRAF task fxcor was used to measure velocity dispersions.

Line-strengths were measured and transformed to the Lick system by closely following procedures outlined in a number of papers (e.g. González 1993; Fisher et al. 1995; Worthey & Ottaviani 1997; Trager et al. 1998; Kuntschner 2000). The spectra were broadened to the Lick resolution ($\sim$9 Å full width at half-maximum) and the line-strengths were measured using the program INDEXF (Cardiel et al. 1998).

A number of corrections were then applied to the measured line-strengths to fully calibrate them to the Lick system. These corrections include a velocity dispersion correction to account for the change in the line-strength caused by velocity broadening, an aperture correction to account for the different linear sizes subtended by the different fibres at different redshifts, and, finally, applying any offsets that may arise due to the fact that the Lick spectra were not flux calibrated. This resulted in the measurement of the line-strength indices $C_2$4668, Hβ, Hβ_G, [O III]$_1$, [O III]$_2$, Fe5015, Mg$_1$, Mg$_2$, Mgb, Fe5270, Fe5335 and Fe5406 of the stellar populations within the inner $\sim$1 kpc of each galaxy.

The age, [Z/H] and [α/Fe] of a galaxy were obtained by comparing our measured line-strengths to the models of Thomas et al. (2003) and accepting the combination of SPPs of the model with the smallest χ^2 (Proctor et al. 2004b). We interpolate the models logarithmically in steps of 0.02 dex in the age and [Z/H], and 0.01 dex in [α/Fe]. Errors on the parameters were estimated by using the constant χ^2 boundaries as confidence limits (see Press et al. 1992).

In summary, we measured velocity dispersions, redshifts and line-strengths for a total of 416 galaxies: 158 of these are early-type galaxies from Coma, A1139, A3558 or A930 that are located within the Abell radius (i.e. at a projected radial distance $\leq 2\,h_{70}^{-1}$ Mpc) and comprise our cluster sample; 87 are early-type galaxies from the outskirts of these clusters at projected radial distances $> 2\,h_{70}^{-1}$ Mpc and comprise the cluster-outskirts sample; 168 galaxies were deemed to be star forming and make up the emission-line sample; the remaining three galaxies lacked the information necessary to classify them as either an early-type or an emission-line galaxy. Of these 416 galaxies, SPPs were estimated for 219, 142 in the cluster sample and 77 in the cluster-outskirts sample.

3 ABSORPTION-LINE ANALYSIS

3.1 Line-strength–σ relations in cluster early-type galaxies

In early-type galaxies, the strengths of certain absorption features are observed to be correlated with the velocity dispersion. Such correlations are important as they provide links between a galaxy's dynamical and chemical evolution, that is, between the galaxy mass, metallicity and abundance ratios.

Historically, the Mg–σ relation was studied using Mg$_2$, which is measured in magnitudes of the absorbed flux. More recent studies (e.g. Colless et al. 1999; Kuntschner et al. 2001) have used Mgb, which is a more reliable index, as it is narrower, but is measured as an equivalent width in Å. These studies converted indices measured in equivalent widths to magnitudes (for the conversion see Colless et al. 1999), primarily to allow comparison with older studies that used Mg$_2$. We continue this practice and indices that have been converted to magnitudes will be denoted with a prime symbol (e.g. Mgb').

The variations in the index line-strengths with the velocity dispersion for the cluster sample are shown in Fig. 1. These plots contain the combined data from all four clusters, as Kolmogorov–Smirnov (KS) 2D two-sample tests indicate consistency of the line-strength–σ distributions between clusters, in that most distributions differed only at the 1–2σ level. That these relations are found to be consistent in the four clusters, which span the ranges of Abell richness classes and Bautz–Morgan (BM) morphologies, is remarkable. This

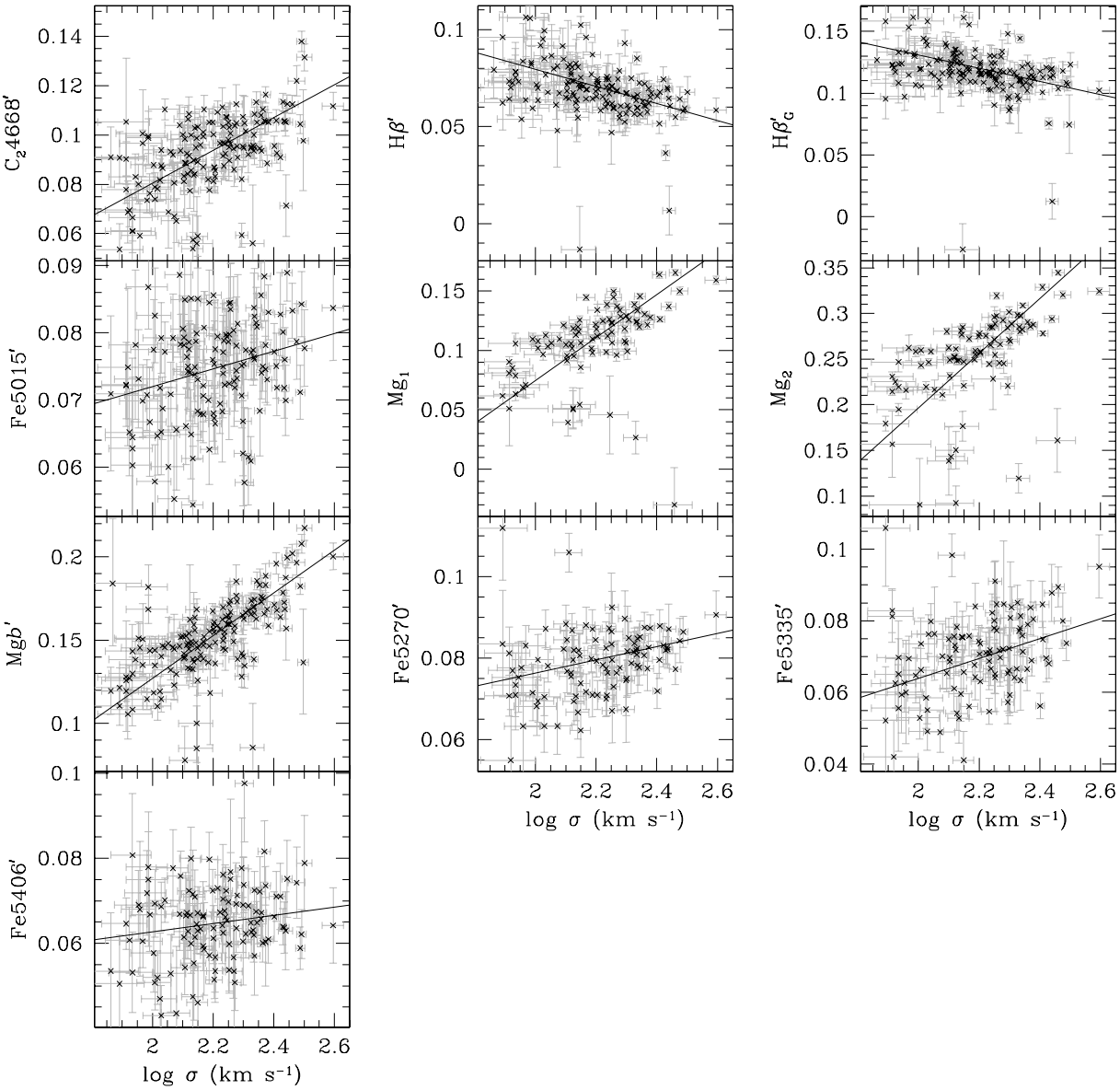

Figure 1. The variations (in magnitudes) in the index line-strengths with the velocity dispersion for the cluster sample. Most indices exhibit a tight relation with strong correlations found for $C_2$4668, Mg_1, Mg_2 and Mgb, while Hβ and Hβ_G exhibit moderate anticorrelations.

suggests that the cluster environment has little effect on the line-strengths of early-type galaxies (see Colless et al. (1999) for a study of the Mg–σ relation as a function of cluster environment). Table 1 shows the results of linear fits to the data, accounting for errors in both quantities, along with the Spearman rank correlation statistic (r_S), the probability that the two quantities are correlated and the estimated intrinsic scatter about each relation.

We assume the intrinsic scatter about these relations is Gaussian and estimate it by maximizing the logarithmic likelihood

$$\log \mathcal{L} = \sum_{i=1}^{n} \log \left[\frac{1}{\sqrt{2\pi\delta_i^2}} \exp\left(\frac{-\Delta I_i^2}{2\delta_i^2} \right) \right], \quad (1)$$

where ΔI_i are the residuals to the fit for index I and $\delta_i^2 = \delta I_i^2 + (a_I\, \delta \log \sigma_i)^2 + \delta_{\rm intr}^2$, where δI_i and $\delta \log \sigma_i$ are the individual errors on the index I and $\log \sigma$, respectively, a_I is the slope of the relation for index I and $\delta_{\rm intr}$ is the estimated intrinsic scatter. These estimated intrinsic scatters are listed in Table 1.

With the exception of Fe5406, correlations are found at $>3\sigma$ confidence level for all indices. Strong correlations ($r_S > 0.5$) are found for $C_2$4668, Mg_1, Mg_2 and Mgb, while a weak correlation ($r_S < 0.3$) is found for Fe5015. Except for Hβ and Hβ_G, which are moderately anticorrelated, all other indices are moderately correlated. The slope of the fit to the Fe5406 data is very flat and consistent with being zero. Hβ and Hβ_G are the only indices used here that are more sensitive to age effects and the only ones that exhibit an anticorrelation; all the other indices are more sensitive to [Z/H] effects and exhibit either a positive correlation or no correlation.

Young stellar populations exhibit strong Balmer absorption features, which weaken with the age. Therefore, a simple interpretation of the anticorrelation of Hβ and Hβ_G with the velocity dispersion is that more massive galaxies are older. The simple interpretation of the positive correlation between the metal-sensitive indices and velocity dispersion is that more massive galaxies are more metal rich. The usual explanation of this trend is that massive galaxies are better able to retain their heavy elements due to their larger gravitational

Table 1. The line-strength–σ fits, Spearman rank correlation statistics, probabilities of a correlation and the intrinsic scatter ($\delta_{\rm intr}$, in mag) for the cluster galaxies.

Index	Zero-point	Slope	$r_{\rm S}$	Probability	$\delta_{\rm intr}$
$C_2 4668'$	-0.053 ± 0.009	0.067 ± 0.004	0.546	1.000	0.0096 ± 0.0011
$H\beta'$	0.167 ± 0.009	-0.044 ± 0.004	-0.479	1.000	0.0075 ± 0.0012
H $\beta'_{\rm G}$	0.238 ± 0.011	-0.054 ± 0.005	-0.442	1.000	0.0120 ± 0.0022
Fe5015′	0.046 ± 0.008	0.013 ± 0.003	0.284	0.999	0.0035 ± 0.0008
Mg_1	-0.285 ± 0.018	0.180 ± 0.008	0.626	1.000	0.0198 ± 0.0021
Mg_2	-0.402 ± 0.032	0.299 ± 0.014	0.662	1.000	0.0200 ± 0.0001
Mgb'	-0.130 ± 0.012	0.129 ± 0.005	0.675	1.000	0.0094 ± 0.0013
Fe5270′	0.044 ± 0.008	0.016 ± 0.004	0.342	0.999	0.0045 ± 0.0012
Fe5335′	0.008 ± 0.011	0.028 ± 0.005	0.352	1.000	0.0081 ± 0.0009
Fe5406′	0.043 ± 0.011	0.010 ± 0.005	0.166	0.921	0.0035 ± 0.0012

potential, a scenario that arises naturally in galactic wind models (e.g. Arimoto & Yoshii 1987). Alternatively, a variable initial mass function could lead to a similar mass–[Z/H] relation. Koeppen, Weidner & Kroupa (2007) have developed a model where the effective upper mass limit of stars is lower in galaxies with a low star formation rate. This reduces the number of Type II supernovae and hence [Z/H] in low-mass galaxies and leads to a similar mass–[Z/H] relation.

We compare our line-strength–σ relations to various estimates from the literature in Table 2. These estimates are based on a sample of early-type galaxies from the Fornax cluster (Kuntschner 2000), a sample of red-sequence galaxies from numerous low-z clusters (Nelan et al. 2005), a magnitude-limited sample of early-type galaxies drawn from the SDSS (Clemens et al. 2006), a sample of early-type galaxies in high-density environments (Sánchez-Blázquez et al. 2006), a magnitude-limited sample of early-type galaxies in high-density environments (Ogando et al. 2008) and a sample of early-type galaxies from the core of the Coma cluster (Matković et al. 2009).

Generally, our results compare well with those in the literature. We find that in the majority of cases the slopes agree at the 2σ level or better. Of those comparisons that disagree by more than 3σ, we note that almost half are comparisons to the estimates of Clemens et al. (2006) and the rest consist almost entirely of comparisons of Mg_1 and Mg_2.

The discrepancy with Clemens et al. (2006) possibly arises due to differences in the aperture corrections applied to each data set. We correct our line-strength measurements to a fixed physical size of $\sim$1 kpc, independent of the velocity dispersion of the galaxy. The correction applied by Clemens et al., however, is to a physical size of $r_{\rm e}/10$ and is a function of the velocity dispersion. Confusing the issue is the fact that some of their slopes are steeper than ours

Table 2. A comparison of our line-strength–σ relations to those found in the literature.

Reference	$C_2 4668'$		$H\beta'$		Fe5015′	
	Zero-point	Slope	Zero-point	Slope	Zero-point	Slope
This study	-0.053 ± 0.009	0.067 ± 0.004	0.167 ± 0.009	-0.044 ± 0.004	0.046 ± 0.008	0.013 ± 0.003
Kuntschner (2000)	-0.110 ± 0.042	0.090 ± 0.018	0.106 ± 0.015	-0.020 ± 0.007	0.002 ± 0.019	0.036 ± 0.008
Nelan et al. (2005)		0.075 ± 0.002		-0.041 ± 0.001		0.015 ± 0.001
Clemens et al. (2006)	0.044 ± 0.003	0.025 ± 0.003	0.227 ± 0.002	-0.071 ± 0.002	0.127 ± 0.002	-0.023 ± 0.002
Sánchez-Blázquez et al. (2006)	-0.071 ± 0.018	0.067 ± 0.008	0.087 ± 0.009	-0.012 ± 0.004	0.025 ± 0.011	0.021 ± 0.005
Ogando et al. (2008)			0.156 ± 0.013	-0.042 ± 0.006	0.053 ± 0.010	0.011 ± 0.004
Matković et al. (2009)	-0.044 ± 0.014	0.060 ± 0.014	0.116 ± 0.009	-0.024 ± 0.009	0.060 ± 0.007	0.005 ± 0.007
Reference	Mg_1		Mg_2		Mgb'	
	Zero-point	Slope	Zero-point	Slope	Zero-point	Slope
This study	-0.285 ± 0.018	0.180 ± 0.008	-0.402 ± 0.032	0.299 ± 0.014	-0.130 ± 0.012	0.129 ± 0.005
Kuntschner (2000)	-0.158 ± 0.035	0.136 ± 0.015	-0.127 ± 0.054	0.191 ± 0.023	-0.056 ± 0.044	0.102 ± 0.020
Nelan et al. (2005)		0.121 ± 0.003		0.189 ± 0.003		0.134 ± 0.002
Clemens et al. (2006)	-0.245 ± 0.010	0.163 ± 0.004	-0.198 ± 0.013	0.208 ± 0.006	-0.155 ± 0.007	0.142 ± 0.007
Sánchez-Blázquez et al. (2006)					-0.050 ± 0.019	0.091 ± 0.008
Ogando et al. (2008)	-0.159 ± 0.020	0.131 ± 0.009	-0.153 ± 0.029	0.194 ± 0.013	-0.095 ± 0.018	0.112 ± 0.008
Matković et al. (2009)	-0.204 ± 0.036	0.141 ± 0.017	-0.143 ± 0.045	0.178 ± 0.020	-0.023 ± 0.015	0.080 ± 0.015
Reference	Fe5270′		Fe5335′		Fe5406′	
	Zero-point	Slope	Zero-point	Slope	Zero-point	Slope
This study	0.044 ± 0.008	0.016 ± 0.004	0.008 ± 0.011	0.028 ± 0.005	0.043 ± 0.011	0.010 ± 0.005
Kuntschner (2000)	0.024 ± 0.020	0.029 ± 0.009	-0.017 ± 0.020	0.043 ± 0.009	0.023 ± 0.026	0.023 ± 0.012
Nelan et al. (2005)		0.017 ± 0.001		0.023 ± 0.001		0.018 ± 0.001
Clemens et al. (2006)	0.085 ± 0.003	-0.001 ± 0.003	0.014 ± 0.003	0.027 ± 0.003	-0.002 ± 0.003	0.031 ± 0.003
Sánchez-Blázquez et al. (2006)	0.027 ± 0.007	0.024 ± 0.003	-0.001 ± 0.013	0.035 ± 0.006		
Ogando et al. (2008)	0.049 ± 0.008	0.015 ± 0.004	0.029 ± 0.009	0.020 ± 0.004	0.034 ± 0.009	0.018 ± 0.004
Matković et al. (2009)	0.092 ± 0.009	-0.007 ± 0.009	0.069 ± 0.008	0.001 ± 0.008		

(e.g. Fe5406), some are shallower (e.g. $C_2$4668) and some are in the opposite sense (e.g. Fe5015).

The discrepancy between our estimated slopes of Mg_1 and Mg_2, and those in the literature is a little easier to understand. Both these indices have very broad definitions and so their line-strengths are highly-sensitive to the shape of the continuum. The fact that we divided out our continuum is probably the reason for this discrepancy. This is one of the reasons why we excluded these two indices from our fits to the models in estimating the SPPs (see section 6 in Paper I).

Most comparisons with Matković et al. (2009) agree at better than the 3σ level, the exceptions being Mg_2 and Mg*b*, but since both samples include early types from the core of the Coma cluster, it is worthwhile to make a direct comparison of these galaxies alone. Overall, this results in better agreement between the slopes, although the change is almost negligible in most cases. Three indices ($C_2$4668, Fe5270 and Fe5335) show worse agreement, but the largest change in significance is only 0.24σ. All other indices show better agreement; again, most changes are small except in the case of Hβ where the significance changes by 1.38σ from 2.03 to 0.65σ.

The intrinsic scatters found for our line-strength–σ relations are given in Table 1. Most of our estimates agree well with those of Kuntschner (2000) and Sánchez-Blázquez et al. (2006), with perhaps the exceptions of Hβ, Fe5015, Fe5270 and Fe5335. We find an intrinsic scatter in Hβ of 0.008 mag (as do Sánchez-Blázquez et al.), which is double that of Kuntschner. For the three Fe indices, our scatters are larger than those found by Sánchez-Blázquez et al. who find negligible to no scatter in these relations. Our estimates for these indices are in good agreement with that of Kuntschner, except for Fe5335 for which we find almost double the scatter of that found by this author (0.008 mag compared to 0.005 mag).

Given that the galaxies from this study are drawn from four different clusters, with varying richness classes and BM classifications, the small intrinsic scatters about the line-strength–σ relations are truly remarkable and imply that the stellar populations in cluster early-type galaxies are homogeneous. This result agrees with that of Colless et al. (1999) who found no correlation between the Mg–σ zero-point and cluster velocity dispersion, X-ray luminosity or X-ray temperature (see also Bernardi et al. 1998; Worthey & Collobert 2003; Sánchez-Blázquez et al. 2006). For galaxies in clusters, Jørgensen, Franx & Kjærgaard (1996) found that the Mg–σ residuals are weakly correlated with the local density. However, since the residuals are correlated with the cluster velocity dispersion and not the projected clustercentric distance, the interpretation is of a correlation between the Mg–σ zero-point and cluster mass, albeit a weak one.

3.2 Line-strengths–σ relations in the cluster outskirts

Using the wide field of the 6dF and, in the cases of A1139 and A930, offsetting the field centres with respect to the cluster centres allowed us to obtain data on galaxies well outside the clusters. We obtained line-strengths of galaxies out to a projected clustercentric radius of $\sim 19\, h_{70}^{-1}$ Mpc, which corresponds to $\sim 10 R_{\rm vir}$. We note that the average distance between Abell clusters is $\sim 30\, h_{70}^{-1}$ Mpc.

The trends with the velocity dispersion of the line-strengths in the cluster-outskirts sample (i.e. those galaxies outside $R_{\rm Abell}$) are shown in Fig. 2. The solid line in each panel is our linear fit to the data (accounting for errors in both quantities), while the dashed line is the fit to the cluster galaxies. In Table 3, we list the details of the fits, the Spearman rank correlation statistics, the probabilities of a correlation and the estimated intrinsic scatters about the relations. The last column in this table shows the number of standard deviations by which the slopes of the cluster-outskirts sample relations differ from the cluster sample relations; all indices are found to have slopes consistent with those found for galaxies in the cluster sample. However, the only indices that show significant correlations at the 3σ level in the cluster-outskirts sample are Mg*b* and H$\beta_{\rm G}$, and while the strength of the correlation remains the same for H$\beta_{\rm G}$, it is reduced for Mg*b* from a strong correlation in the cluster sample to a moderate correlation here.

The change in the Fe indices is interesting. Fe5015 changes from being weakly correlated in the cluster sample to uncorrelated in the cluster-outskirts sample. The other three Fe indices remain moderately-to-weakly correlated (although with reduced significance), but their slopes are all consistent with being zero. In the cluster sample, only Fe5406 had a slope that was consistent with being zero. In addition, all four Fe indices have decreased intrinsic scatters about their fits, as does Mg_1. $C_2$4668, Hβ, H$\beta_{\rm G}$ and Mg*b* all show an increase in the intrinsic scatter, while for Mg_2 it remains the same.

There appears to be a large number of galaxies that have low index strengths compared to those expected from the relations found in the cluster sample. For Fe5015, the spread is consistent with what is found in the cluster sample. The galaxies with low Hβ and H$\beta_{\rm G}$ strengths, which also are found in the cluster sample but in smaller numbers, are possibly those that suffer from the nebular in-fill. Most of the galaxies in the cluster-outskirts sample were observed with the 6dF and so have no details of the Hα emission because the wavelength coverage was insufficient. Therefore, it is not unexpected that the level of this possible contamination by star-forming galaxies in this sample is slightly higher than in the cluster sample.

In the cases of $C_2$4668′ and Mg*b*, there does appear to be a real subpopulation of galaxies that are genuinely offset from the relations found in the cluster sample, having weaker line-strengths for a given velocity dispersion. This is possible if galaxies in clusters find it easier to retain their heavier elements than those in their outskirts, due to the dense intracluster medium retarding the development of galactic winds and the expulsion of the heavier elements.

Another possibility is that the weakened line-strengths are caused by the aperture correction. Early-type galaxies exhibit strong metallicity and age gradients (e.g. Davies, Sadler & Peletier 1993) and indices measured in massive galaxies will sample a smaller fraction of the effective radius than those in less-massive galaxies. If lower mass galaxies are found preferentially in the cluster outskirts, then this could lead to a change in the relations in the two regions. These aperture corrections are necessary to allow a fair comparison between galaxies in clusters at different redshifts and between galaxies in the same cluster but observed with fibres that subtend different angles (2dF $\sim$ 2.1 arcsec and 6dF $\sim$ 6.7 arcsec). However, we do not find that lower mass galaxies are preferentially found in the cluster-outskirts sample. In fact, while the distributions of magnitudes are similar in shape in both regions (because we deliberately targeted brighter galaxies), the peak of the distribution in the core is shifted to fainter magnitudes relative to the cluster-outskirts sample by $\sim$1 mag, that is, on average, the cluster-outskirts galaxies are brighter. Therefore, this cannot be the reason for the weakening of the relations.

3.3 The radial distribution of star-forming galaxies in clusters

In the analyses so far, the included galaxies were limited to those that showed no significant sign of ongoing star formation, as

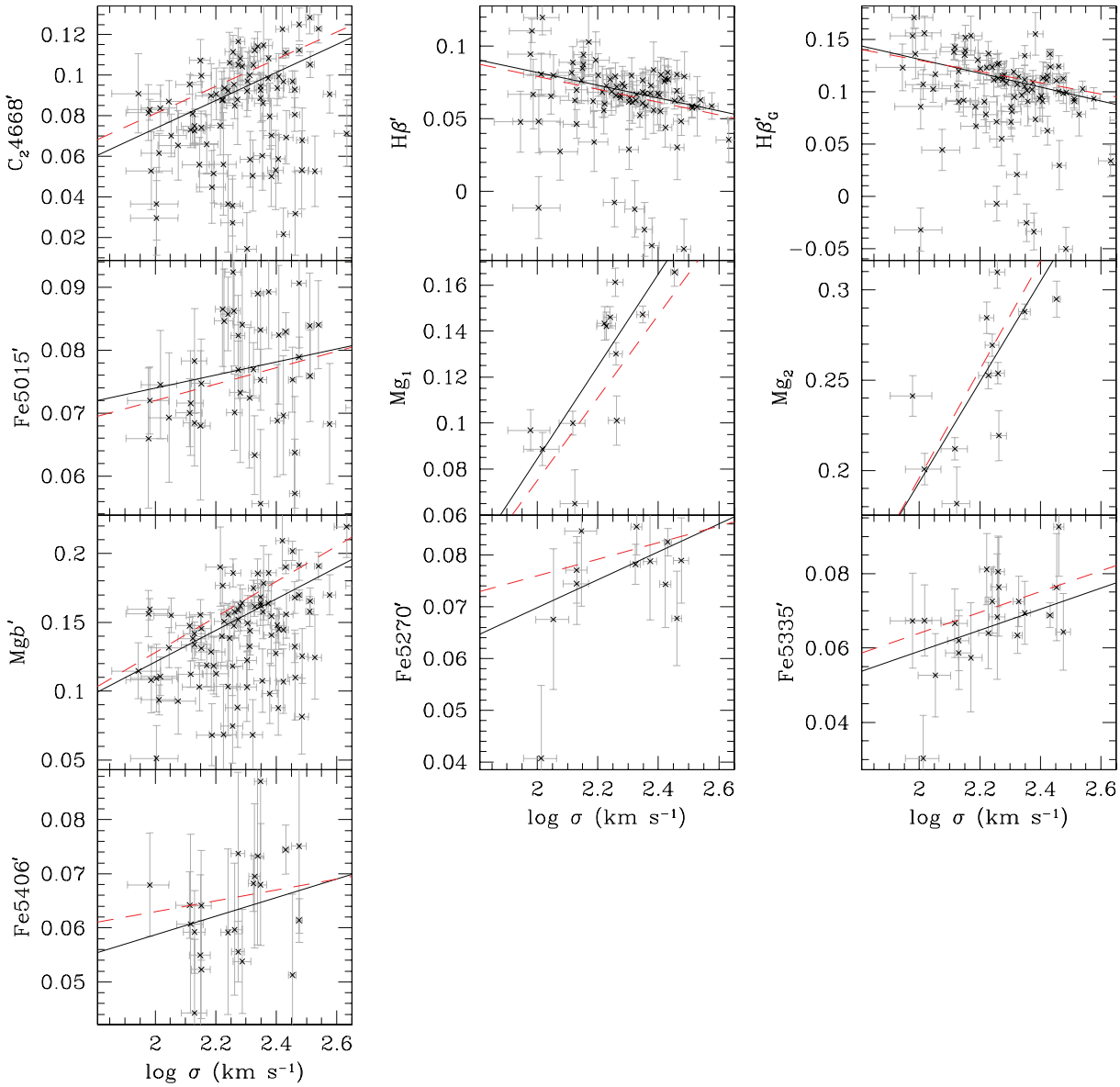

Figure 2. The variations (in magnitudes) in the index line-strengths with the velocity dispersion for the cluster-outskirts sample. The solid line is the linear fit to the data, while the dashed red line is the fit to the cluster sample. The slopes of all relations are consistent with those found in the cluster sample.

Table 3. The line-strength–σ fits, Spearman rank correlation statistics (r_S), probabilities of a correlation and intrinsic scatters (δ_{intr}; in mag) for galaxies in the cluster-outskirts sample. The number of standard deviations by which the slopes of the cluster-outskirts sample relations differ from the cluster sample relations (σ_{diff}) is given in the last column.

Index	Zero-point	Slope	r_S	Probability	δ_{intr}	σ_{diff}
$C_2 4668'$	-0.064 ± 0.017	0.069 ± 0.007	0.260	0.985	0.0200 ± 0.0020	0.3
$H\beta'$	0.171 ± 0.017	-0.044 ± 0.007	-0.275	0.988	0.0184 ± 0.0045	0.0
$H\,\beta'_G$	0.264 ± 0.021	-0.066 ± 0.009	-0.322	0.997	0.0200 ± 0.0003	1.2
Fe5015′	0.053 ± 0.016	0.010 ± 0.007	0.086	0.413	0.0029 ± 0.0018	0.4
Mg_1	-0.316 ± 0.056	0.200 ± 0.024	0.748	0.995	0.0142 ± 0.0038	0.8
Mg_2	-0.363 ± 0.078	0.278 ± 0.034	0.650	0.978	0.0200 ± 0.0036	0.6
Mgb'	-0.108 ± 0.023	0.115 ± 0.010	0.392	1.000	0.0200 ± 0.0012	1.3
Fe5270′	0.016 ± 0.035	0.027 ± 0.015	0.410	0.814	0.0000 ± 0.0011	0.7
Fe5335′	0.003 ± 0.030	0.028 ± 0.013	0.548	0.990	0.0000 ± 0.0020	0.0
Fe5406′	0.024 ± 0.030	0.017 ± 0.013	0.405	0.939	0.0027 ± 0.0017	0.5

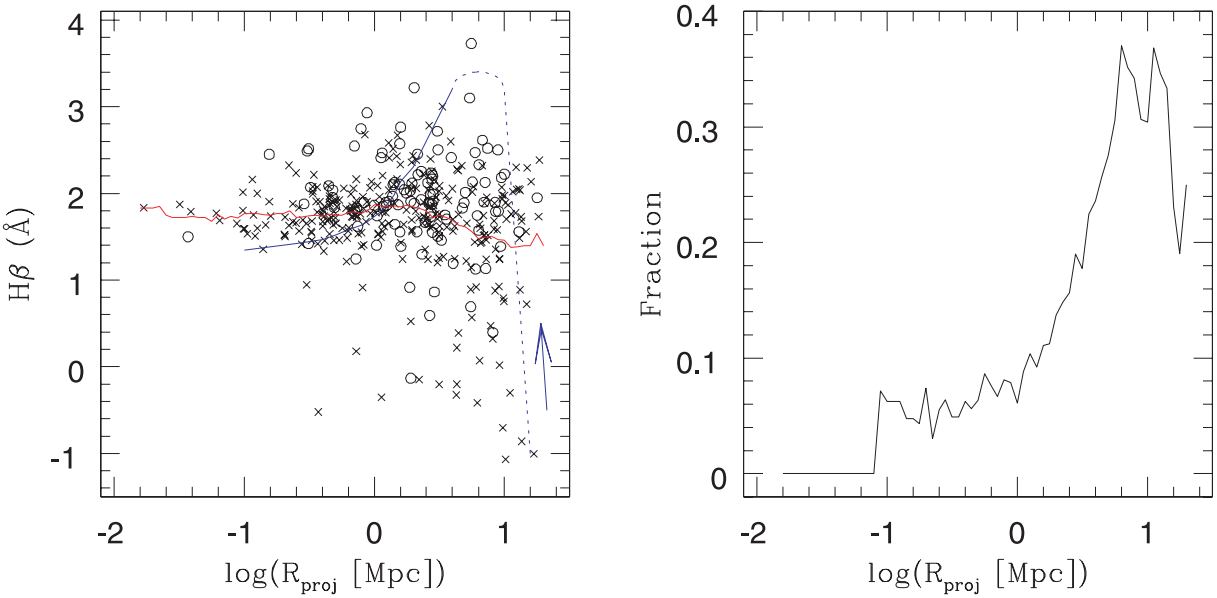

Figure 3. Left-hand panel: the variation in the Hβ line-strength as a function of the projected clustercentric radius. The circles represent early-type galaxies and the crosses represent galaxies that are classified as emission-line galaxies. The red line shows how the mean Hβ line-strength changes with the radius and indicates that on average galaxies in the outskirts of clusters are ∼0.4 Å weaker in Hβ than those in the centre of clusters. The blue line shows how the Hβ line-strength evolves in a galaxy as it ages after an instantaneous burst of star formation (the direction is given by the blue arrow; see text for details). Right-hand panel: the fraction of galaxies with H$\beta \leq 1.4$ Å as a function of the projected clustercentric radius.

determined from Hα or [O III] λ5007 Å emissions. This allows us to be reasonably confident that their Hβ absorption feature is free from the in-filling caused by nebular emissions. However, from these previously excluded galaxies, we can determine where in the cluster and its surrounds star-forming galaxies reside.

In the left-hand panel of Fig. 3, we show, for our entire sample of galaxies, the Hβ line-strengths as a function of the projected clustercentric distance. The circles represent galaxies that are classified as early types, while the crosses represent emission-line galaxies (and were up to this point excluded from our analysis). The distribution of Hβ line-strengths forms a ridge at ∼1.8 Å. Most of the galaxies with Hβ line-strengths weaker than ∼1.4 Å are those classified as emission-line galaxies, although a few galaxies classified as early types also lie below this ridge line. It is possible that these galaxies have weak Hβ due to the in-filling and yet show no significant sign of the [O III] λ5007Å emission. This confirms that while correcting for the Hβ emission by the strength of the [O III] λ5007Å emission line (González 1993; Trager et al. 2000a,b) may be acceptable in a statistical sense; it is not reliably applicable to individual galaxies, which may show moderate to strong Hβ emission and little or no [O III] λ5007Å emission (Nelan et al. 2005).

Fig. 3 shows an increasing scatter in Hβ line-strengths with increasing radius. Not only is there a scatter to lower values (an indication of older ages or possibly the Hβ in-filling in galaxies that have experienced recent star formation), but there is also a scatter to higher values, and thus younger ages, for early-type galaxies. The red line in the left-hand panel of Fig. 3 shows how the mean Hβ line-strength (calculated for galaxies within a 0.4 dex radius bin at steps of 0.05 dex) changes with the radius. We see that within a radius of $\sim 2\, h_{70}^{-1}$ Mpc (i.e. $\sim R_{\rm Abell}$) the mean value is a constant (∼1.8 Å), while outside this radius, it steadily decreases to a value of ∼1.4 Å. Since the oldest isochrone (15 Gyr) in the Thomas et al. (2003) models has Hβ strengths ∼1.6–2 Å, we conclude that these low line-strengths, for the galaxies classified as early types, represent the nebular in-fill in recently star-forming galaxies, which are preferentially found in the outer regions of the cluster environment. This conclusion is consistent with a previous study of the galaxy star formation rate and environment by Lewis et al. (2002), which found increasing star formation rates with increasing distance from the cluster centre that converge to field rates at distances greater than $\sim 3R_{\rm vir}$ (see also Gómez et al. 2003; Kauffmann et al. 2004).

The distribution of galaxies in this figure can be thought of as tracking the evolution of a star-forming galaxy. A galaxy falling into the cluster undergoes a burst of star formation, which shifts the galaxy to the Hβ emission (i.e. negative line-strengths). As the episode of the star formation progresses and the galaxy moves deeper into the cluster, the galaxy gradually shifts to stronger Hβ absorption (positive line-strengths). Then, once star formation has ceased, the galaxy settles back on to the ridge. This evolution is represented schematically by the blue line in the figure. The dotted segment of the line represents the galaxy as it moves from being a star-forming galaxy to a post-starburst galaxy (the Hβ emission line-strengths are indicative only). The solid segment of the line shows how, according to the Thomas et al. models, the Hβ line-strength changes in a galaxy with [Z/H] = 0.35 dex and [α/Fe] = 0.2 dex as it ages from 1 to 15 Gyr. The mapping between the projected clustercentric radius and time is arbitrary. This figure is similar to fig. 10 in Couch & Sharples (1987), which shows the evolutionary track of a star-bursting galaxy in the Hδ–colour space.

The right-hand panel of Fig. 3 shows the fraction of galaxies (in the same bins as used for calculating the mean in the left-hand panel) that have line-strengths less than 1.4 Å. In the core of the cluster, none of the galaxies fall below this value, while at large radii the fraction increases rapidly to the limit of our data, where ∼40 per cent of galaxies have line-strengths less than this value. We conclude that the cluster core is relatively free from young galaxies and galaxies that have experienced recent star formation, and that these galaxies are found more commonly outside $R_{\rm Abell}$.

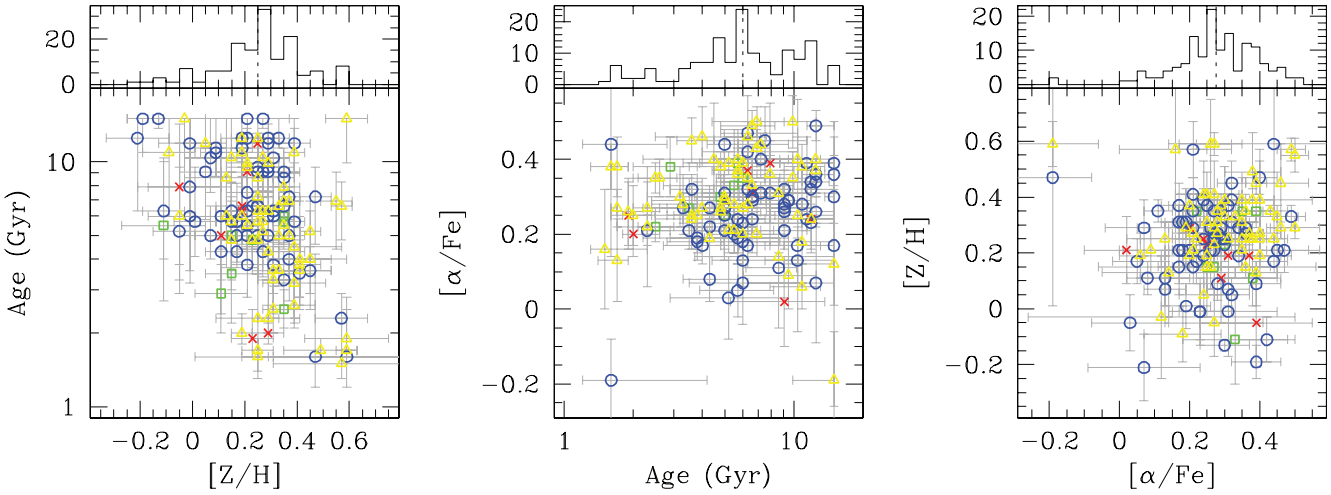

Figure 4. The distributions of the SPPs for all galaxies in the cluster sample. Marginal distributions are shown for each parameter and the dotted lines show the median values of each parameter. Galaxies from Coma are shown as blue circles, from A1139 as green squares, from A3558 as yellow triangles and from A930 as red crosses.

4 STELLAR POPULATION PARAMETER DISTRIBUTIONS

4.1 The cluster distributions

The distributions of SPPs from the four clusters combined are shown in Fig. 4. Marginal distributions are plotted for each of the parameters and the median values are marked as dotted lines. Galaxies from Coma are shown as the blue circles, from A1139 as the green squares, from A3558 as the yellow triangles and from A930 as the red crosses. Errors are shown for individual galaxies, but two points must be kept in mind. First, the age and [Z/H] errors are correlated and so the error bars here do not accurately reflect the true shape of the confidence contours. For the two other combinations of parameters, the errors are much less correlated and so the error bars are a good representation of the confidence contours (see Paper I). Secondly, a galaxy's error estimate cannot be larger than its distance to the edge of the model grid. This is only an issue for age estimates since we quote two-sided errors. So, if a galaxy's error bar reaches 15 Gyr, then it should be considered a lower limit only.

Looking at the distributions as a whole, we note that very few galaxies have [Z/H] less than solar with most having $0.1 \lesssim [Z/H] \lesssim 0.4$ dex. Similarly, [α/Fe] is mostly greater than solar and lies in the range $0.2 \lesssim [\alpha/Fe] \lesssim 0.4$ dex. The bulk of the galaxies have old ages and almost all lie in the range $4 \lesssim$ age $\lesssim 15$ Gyr. The distributions we find for the cluster sample are in general agreement with those found by previous authors (e.g. González 1993; Jørgensen 1999a; Kuntschner 2000; Trager et al. 2000b; Poggianti et al. 2001; Thomas et al. 2005; Collobert et al. 2006).

Looking at the SPP distributions of each cluster individually, we find few differences. The median values and errors for the SPPs in each cluster are given in Table 4. The errors on the median values were estimated from Monte Carlo bootstrap simulations in the following manner. For each galaxy in a cluster, we randomly draw index values from the galaxy's index error distributions, using the same set of indices that were used to estimate the parameters originally. These index values are then converted to parameter estimates and the median values are determined. This process is repeated 10 000 times and the rms errors on the median values are computed.

The distributions of SPPs from cluster to cluster show remarkable similarity, with no significant differences between the median values of any of the four clusters. However, to conclusively detect any differences in the age and [Z/H] distributions, a two-sample 2D KS test is required, due to the correlated errors between the age and [Z/H]. For the [α/Fe] distributions, a two-sample 1D KS test is sufficient. The results of these tests are that the joint distributions of the age and [Z/H], and the distributions of [α/Fe] in each of the four clusters are consistent with each other.

Table 4. The median SPP values for each cluster and the number of galaxies for which the parameters were measured.

Cluster	[Z/H]	Age	[α/Fe]	N_{gal}
Coma	0.25 ± 0.02	6.6 ± 0.6	0.27 ± 0.01	65
A1139	0.19 ± 0.08	4.9 ± 1.6	0.32 ± 0.04	8
A3558	0.29 ± 0.04	5.7 ± 0.9	0.29 ± 0.02	61
A930	0.20 ± 0.08	6.4 ± 2.1	0.27 ± 0.05	8

Looking at the combined distributions of the cluster sample (142 galaxies in total), we find that the median [Z/H] is 0.25 ± 0.14 dex, the median age is $6.0^{+4.6}_{-2.6}$ Gyr and the median [α/Fe] is 0.28 ± 0.11 dex. The errors on these median values were determined the same way as for the clusters individually. These median values are shown as the dotted lines in the marginal distributions in Fig. 4.

There are some galaxies that have line-strengths that fall outside the ranges predicted by the stellar population models, in that there are six galaxies with age = 15 Gyr, four with [Z/H] = 0.59 dex and two with [α/Fe] = −0.19 dex. Two galaxies have more than one parameter on the edge of the models and so in total there are 10 such galaxies. These galaxies are assigned the combination of SPPs that most nearly fits the combination of line-strengths, as mentioned in Paper I. It is hard to determine the origin of this difference between the data and the models, which could be due to errors in the stellar population models (it should be noted that the models provide no estimate of systematic uncertainties) or due to errors in the observations or data reduction; only a small percentage of galaxies are affected, with ∼90 per cent of galaxies having self-consistent model parameter fits.

For the galaxies with age = 15 Gyr, it is possible that some of these galaxies are affected by the nebular Hβ emission, despite the fact that care was taken in eliminating such galaxies. As was noted

in Paper I, it is possible for galaxies to have Hβ in emission and no detectable [O III] λ5007 Å (Nelan et al. 2005). If this Hβ emission is undetectable, because it is swamped by the Hβ absorption, and there is no [O III] λ5007 Å emission, then such a galaxy will not be classified as an emission-line galaxy and will not be excluded from the cluster sample.

It is also evident that there appears to be an anticorrelation between [Z/H] and the age, in the sense that younger galaxies are more metal rich. This might, in principle, be due to the non-orthogonal nature of the [Z/H]–age grids produced by the stellar population models, which mean that the errors on these two quantities are correlated. The effect is that an increase in a [Z/H]-sensitive index results not only in an increase in [Z/H], but also in a decrease in the age; correspondingly, an increase in an age-sensitive index results in a decrease in the age and an increase in [Z/H]. Due to the irregular shape of the grid, this effect varies with the location over the grid.

That a degree of anticorrelation between the age and [Z/H] is introduced by the correlated errors is not disputed; however, whether this accounts for the anticorrelation entirely is still contentious (Colless et al. 1999; Jørgensen 1999a; Trager et al. 2000a; Kuntschner et al. 2001; Poggianti et al. 2001; Proctor & Sansom 2002; Terlevich & Forbes 2002; Bernardi et al. 2005; Sánchez-Blázquez et al. 2006). Some studies find that there exists a moderate anticorrelation over and above that introduced by the errors (e.g. Colless et al. 1999), while others find that no correlation exists once the errors are taken into account (e.g. Kuntschner et al. 2001). To determine whether the anticorrelation between the age and [Z/H] is real or not, we perform a simple test which involves comparing the degree of anticorrelation in the observed joint age–[Z/H] distribution with those obtained by Monte Carlo simulations.

Due to the need for an automated process to convert SPPs to line-strengths (and vice versa), it is not feasible to use the method of SPP estimation that makes use of all available indices. Therefore, for this exercise, we rely on only three indices, Hβ, Mgb and Fe5335. Combinations of these three indices are commonly used in line-diagnostic diagrams to estimate SSPs. With this combination of indices, the age distribution is approximately exponential and both the [Z/H] and [α/Fe] distributions are approximately Gaussian (see Fig. 5).

We start by generating a sample of galaxies with age, [Z/H] and [α/Fe] estimates (parameter triples); the [Z/H] and [α/Fe] estimates were drawn from the distributions defined by the medians of the observed values and their intrinsic scatters and the age estimates were drawn from an exponential distribution (see Section 6 for details on how the intrinsic scatters and the e-folding of the exponential age distribution were determined). These parameter triples are then converted to Hβ, Mgb and Fe5335 index values (index triples), which are then perturbed using the observed index error distributions. These perturbed index triples are then converted back to parameter triples and the Spearman rank correlation statistic r_S is calculated for the age and [Z/H]. This procedure is carried out 10 000 times. From these Monte Carlo simulations, we determine the probability of obtaining by chance a correlation greater than that found for the observed data and we find that there exists a real anticorrelation between the age and [Z/H] (over and above the error-induced correlation) that is significant at the $>3\sigma$ level.

4.2 The distributions in the cluster outskirts

The distributions of SPPs in the cluster-outskirts sample (red crosses) are compared to those from the clusters (black circles) in Fig. 6. For the sake of clarity, only the errors for the cluster-outskirts sample are shown. The dashed lines in the marginal distributions are the median galaxy parameters for the cluster-outskirts sample and the dotted lines are for the cluster sample. The galaxies in the cluster-outskirts sample have a median [Z/H] of 0.21 ± 0.27 dex, a median age of $6.6^{+8.1}_{-3.6}$ Gyr and a median [α/Fe] of 0.27 ± 0.21 dex. Compared to the combined cluster sample, we detect no difference in the median values for the galaxy parameters, although the errors are substantial.

Looking at the distributions we see that there is very little difference between the galaxies in this sample and those in the clusters, an assessment that is confirmed by KS testing (a two-sample 2D KS test in the case of the age and [Z/H] distributions and a two-sample 1D KS test for the [α/Fe] distributions).

The fact that the [α/Fe] distributions are the same in the clusters and their outskirts is intriguing, given that the cores of galaxy clusters are thought to result from regions of high overdensity where the process of the star formation occurs rapidly (Kauffmann & Charlot 1998; Romeo, Portinari & Sommer-Larsen 2005; Schindler et al. 2005; De Lucia et al. 2006). Our result is, however, in agreement with previous studies on [α/Fe] in low- and high-density environments (Kuntschner et al. 2002; Thomas et al. 2005). These results suggest that, in all environments, elliptical galaxies form on similar time-scales.

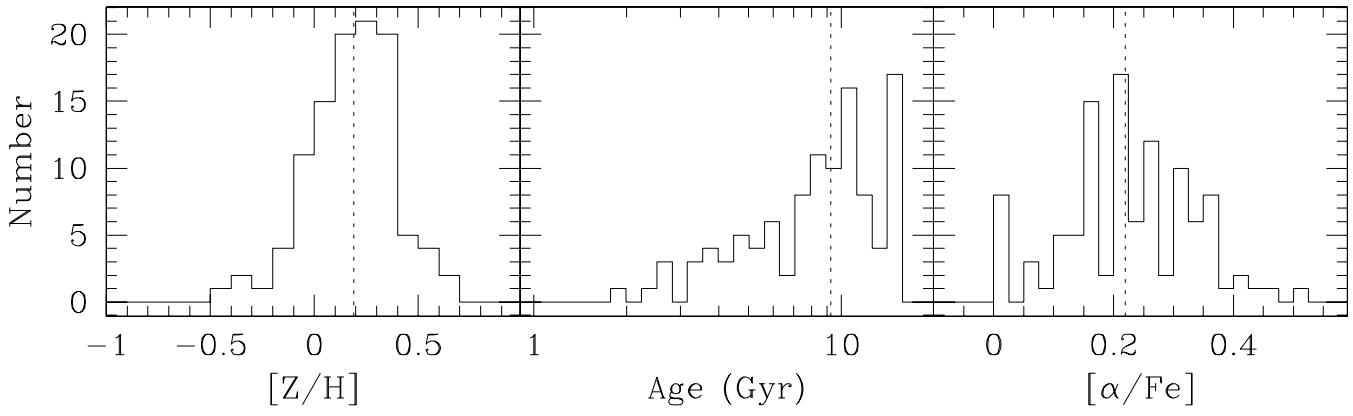

Figure 5. The distributions of the SPPs, estimated from Hβ, Mgb and Fe5335 only, for all galaxies in the cluster sample. The dotted lines show the median values of each parameter.

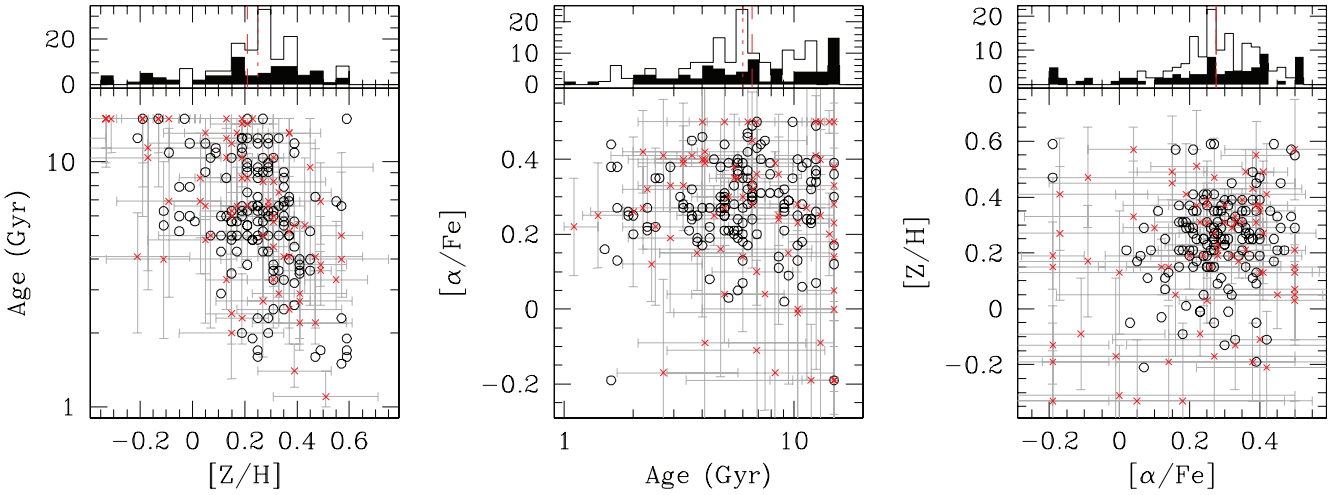

Figure 6. Comparison of the SPPs in the cluster-outskirts sample (black circles) to those in the cluster sample (red crosses). The marginal distributions for the cluster sample are shown as open histograms and for the cluster-outskirts sample as black histograms. The dashed line in the marginal distributions represents the median parameter values in the cluster-outskirts sample and the dotted line represents that of the cluster sample.

The often-found differences in low- and high-density environments between the age (Trager et al. 2000a; Poggianti et al. 2001; Kuntschner et al. 2002; Terlevich & Forbes 2002; Caldwell et al. 2003; Proctor et al. 2004a; Thomas et al. 2005) and [Z/H] (Kuntschner et al. 2002; Thomas et al. 2005), with galaxies on average being ∼2 Gyr younger and more metal rich in lower-density environments, are not reproduced here. Although, given the size of our errors, it is not surprising that we do not detect such a small difference. These results are usually found by comparing truly isolated galaxies with cluster galaxies. As the galaxies in the cluster-outskirts sample are actually drawn from the outer regions of the clusters and the structures surrounding them (out to a projected radial distance of $\sim 19\,h_{70}^{-1}$ Mpc or $\sim 10 R_{\rm vir}$), it is possible that the contrast between the average densities of each environment is not sufficient to reveal any differences in the stellar populations and that the change occurs at a lower density threshold (e.g. between isolated galaxies and those in groups/filaments).

Fig. 7 shows the variations in the SPPs with the projected cluster-centric distance, normalized to the cluster virial radius ($R_{\rm vir}$). The lines in these plots show the mean values in bins containing 15 galaxies extending out to almost $10R_{\rm vir}$. The error bars show the standard error of the mean within each bin. We find no evidence of any significant trends, although it does appear as if [α/Fe] and the age increase moving towards the centre of the cluster, implying that the galaxies in the cluster cores are older and have shorter star formation time-scales than those in the cluster outskirts. Despite the lack of clear trends, there are two other interesting aspects of these plots. First, there appears to be a decrease in [Z/H] outside $\sim 2R_{\rm vir}$. Secondly, at a distance slightly less than the cluster virial radius, there appears to be a dip in the average age. Such a dip would be expected in a scenario where the interaction with the intracluster medium triggers the star formation in an in-falling galaxy, resulting in a stellar population characterized by a young age and extended star-formation time-scale. This decrease in the age begins at a radius $>3R_{\rm vir}$, suggesting that the influence of the cluster extends to large distances. We also note that all galaxies with ages $\lesssim$2 Gyr are located near $R_{\rm vir}$ and the age of the youngest stellar population at a given radius increases moving towards the cluster core.

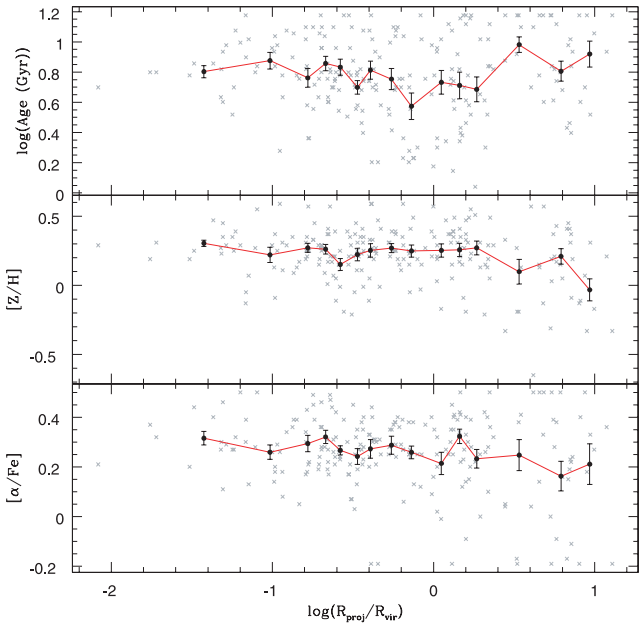

Figure 7. The trend of the mean age (top panel), mean [Z/H] (middle panel) and mean [α/Fe] (bottom panel) as a function of the cluster virial radius. The mean is calculated in bins containing 15 galaxies.

5 THE PARAMETER–σ RELATIONS

5.1 The cluster relations

The variations in the SPPs with the velocity dispersion are shown in Fig. 8. All parameters are found to be moderately correlated with a high level of significance; $>5\sigma$ for log (age) and $>4\sigma$ for [Z/H] and [α/Fe]. Performing linear fits to the relations, we find

$$\log(\text{age}) = (0.64 \pm 0.12)\log\sigma - (0.63 \pm 0.26), \quad (2)$$

$$[\text{Z/H}] = (0.40 \pm 0.08)\log\sigma - (0.63 \pm 0.17), \quad (3)$$

$$[\alpha/\text{Fe}] = (0.20 \pm 0.06)\log\sigma - (0.17 \pm 0.13). \quad (4)$$

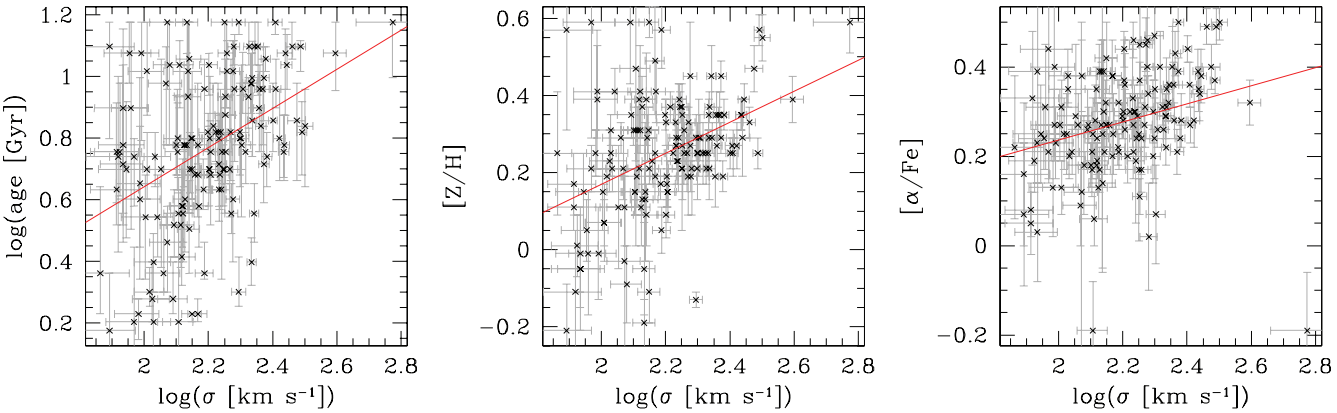

Figure 8. The variations in the SPPs log (age) (left-hand panel), [Z/H] (middle panel) and [α/Fe] (right-hand panel) with log σ of the galaxies in the cluster sample. All three parameters are moderately correlated with log σ. The red line in each panel is the linear fit to the data.

These fits are shown as red lines in Fig. 8. While these results confirm the existence of the [Z/H]–σ and [α/Fe]–σ relations, the correlation of the age with the velocity dispersion found here is not so well accepted (see Section 1 for references).

The behaviour of the age and [α/Fe] with the velocity dispersion is reminiscent of downsizing (Cowie et al. 1996), where the typical mass of a star-forming galaxy increases with the redshift. Looking at the distribution of ages, we see that at all velocity dispersions there exist galaxies with very old stellar populations, but the age of the youngest galaxy at a given velocity dispersion increases with the velocity dispersion. The peak epoch of the star formation in more massive galaxies thus occurred at higher redshifts.

Assuming that the scatter about the relations is Gaussian, we find that the intrinsic scatter in log (age) is 0.20 ± 0.02 dex, in [Z/H] is 0.10 ± 0.02 dex and in [α/Fe] is 0.07 ± 0.01. The uncertainty in these scatters was determined via Monte Carlo simulations. Considering the mean observational errors 0.14, 0.08 and 0.08 dex, respectively, the tightness of these relations is remarkable and shows that the velocity dispersion is an excellent indicator of the SPPs in early-type galaxies, with more massive galaxies being older, more metal rich and having shorter star formation time-scales than less-massive galaxies.

Table 5 lists the SPP–σ relations found in this work and in the literature. The literature estimates come from a sample of early-type galaxies in high-density environments (Thomas et al. 2005), a sample of red-sequence galaxies in low-z clusters (Nelan et al. 2005), a sample of early-type galaxies in high-density environments from the SDSS (Bernardi et al. 2006), a sample of red-sequence galaxies in low-z clusters (Smith et al. 2006), a sample of red-sequence galaxies drawn from the SDSS (Graves et al. 2007), a sample of galaxies from the Shapley supercluster with $\sigma > 100\,\mathrm{km\,s^{-1}}$ (Smith et al. 2007) and a sample of red sequence galaxies in all environments.

Overall, the slopes found here agree well with those found in the literature. The slope of our log (age)–σ relation is consistent with most estimates in the literature except for that of Thomas et al. (2005), which is only a third as steep as ours, and that of Bernardi et al. (2006) who find a slope twice as steep. The existence of a correlation between the age and velocity dispersion is still being debated and this is reflected in the large variation in slopes found in the literature. A possible cause for this is the difficulty in accurately determining ages with the current set of models. The slope of our [Z/H]–σ relation agrees well with those found in the literature, with exceptions of Graves et al. (2007) and Thomas et al. (2010) who find a slope twice and 50 per cent as steep, respectively. The slope of our [α/Fe]–σ relation is consistent with all of the literature values, despite being the smallest.

5.2 The relations in the cluster-outskirts sample

The median values of the SPPs were found to be the same in both the cluster sample and the cluster-outskirts sample, as were the SPP distributions. In order to make a true comparison, one that is free from any biases introduced by the two velocity dispersion distributions, we now compare the parameter–σ relations found in the cluster sample with those in the cluster-outskirts sample.

Table 5. Comparison of the SPP–σ relations from this study with those in the literature.

Reference	log (age)		[Z/H]		[α/Fe]	
	Zero-point	Slope	Zero-point	Slope	Zero-point	Slope
This study						
Cluster	−0.63 ± 0.26	0.64 ± 0.12	−0.63 ± 0.17	0.40 ± 0.08	−0.17 ± 0.13	0.20 ± 0.06
Cluster outskirts	−0.43 ± 0.45	0.54 ± 0.20	−0.24 ± 0.40	0.18 ± 0.18	−0.52 ± 0.31	0.33 ± 0.14
Thomas et al. (2005)	0.46	0.24	−1.06	0.55	−0.42	0.28
Nelan et al. (2005)		0.59 ± 0.13		0.53 ± 0.08		0.31 ± 0.06
Bernardi et al. (2006)	−1.72 ± 0.31	1.15	−0.64 ± 0.01	0.38	−0.54 ± 0.01	0.32
Smith et al. (2006)		0.72 ± 0.14		0.37 ± 0.08		0.35 ± 0.07
Graves et al. (2007)		0.35 ± 0.03		0.79 ± 0.05		0.36 ± 0.04
Smith, Lucey & Hudson (2007)		0.64 ± 0.12		0.38 ± 0.09		0.36 ± 0.07
Thomas et al. (2010)	−0.11 ± 0.05	0.47 ± 0.02	−1.34 ± 0.04	0.65 ± 0.02	−0.55 ± 0.02	0.33 ± 0.01

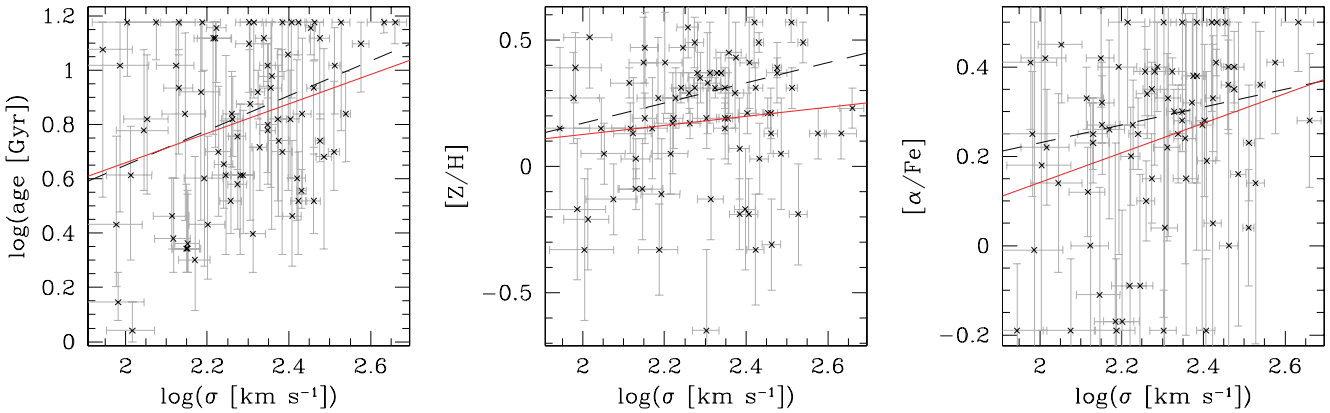

Figure 9. The parameter–σ relations for the cluster-outskirts sample. The solid red lines are the linear fits to the cluster-outskirts sample and the dashed black lines are the linear fits to the cluster sample.

Fig. 9 shows the parameter–σ relations for the galaxies in the cluster-outskirts sample (solid red lines) compared with those in the cluster sample (dashed black lines). Details of the fits are given in Table 5.

None of the SPPs is found to be significantly correlated with the velocity dispersion in the cluster-outskirts sample. Note that the parameter errors are larger in the cluster-outskirts sample than in the cluster sample. This is due to the fact that the galaxies in the cluster outskirts were observed with the 6dF, which has less wavelength coverage than the 2dF, and therefore their SPPs were estimated, on average, from fewer indices. It is possible that these larger errors blur any correlation that may exist.

It is also possible that the change in the number and combination of indices used to estimate the SPPs in the cluster-outskirts sample, when compared to the cluster sample, is the reason why no correlations are found in the former. We therefore check this effect by re-estimating the SPPs of the cluster sample using only Hβ, Mgb and Fe5335. Using these estimates we find that all three parameters are still correlated with the velocity dispersion and that the slopes of both relations are consistent within the errors. Therefore, it is unlikely that the lack of correlations in the cluster-outskirts sample is a result of the change in the number of indices used. We would like to point out that a fit (using the unrestricted set of indices) was only accepted if Hβ was used and at least two other indices. See Paper I for more details.

We show the results of comparing the two sets of estimates in Fig. 10. For [Z/H] and [α/Fe], the agreement between the two sets of estimates is quite good, although there is an offset of 0.05 dex in [α/Fe] in the sense that the unrestricted set of indices gives larger values of [α/Fe]. There is also an offset of 1.3 Gyr between the two age estimates (but in the opposite sense to that of the [α/Fe] offset) and there is some scatter that increases with the age. This is due to the fact that, in index space, the distance between lines of constant age decreases with increasing age so that small shifts in index strengths can lead to large changes in age estimates. According to a Spearman rank correlation test, the two data sets are consistent. This implies that the two ways of measuring the SPPs rank the objects in the same order and that there should be no effect on our results.

6 THE SCATTER IN THE PARAMETER DISTRIBUTIONS IN CLUSTERS

In part, the spread in the SPP distributions found for the cluster sample is due to a combination of our observational errors and the correlations with velocity dispersion. To determine the amount of the intrinsic scatter in the distributions, over and above that caused by the observational errors, we ran a series of numerical simulations. The method used was as follows.

Due to the need to create a large number of models containing a large number of galaxies, which need to have their SPPs converted

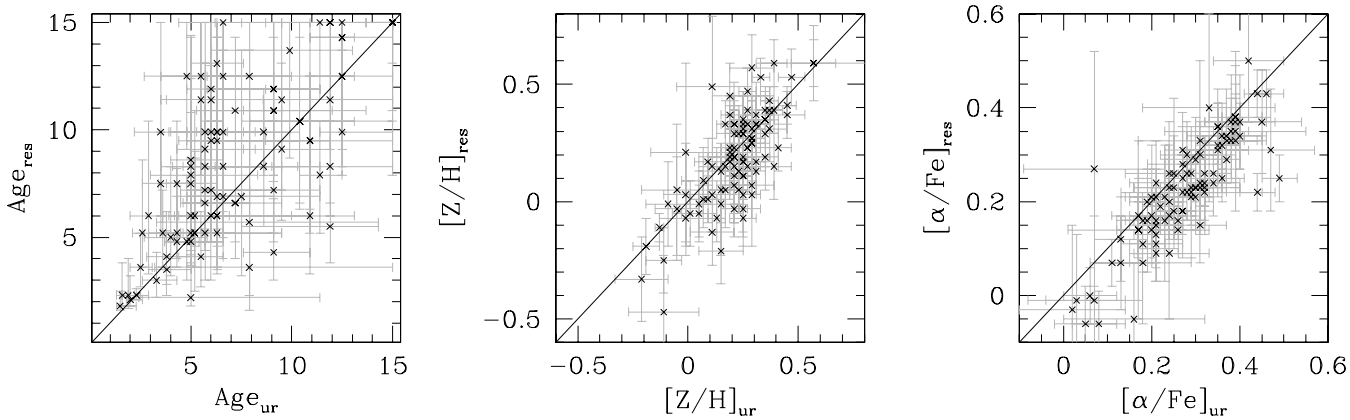

Figure 10. Comparison of the age (left-hand), [Z/H] (middle panel) and [α/Fe] (right-hand panel) estimates obtained from using the restricted and unrestricted set of indices. The solid lines represent the one-to-one relation (see the text for details).

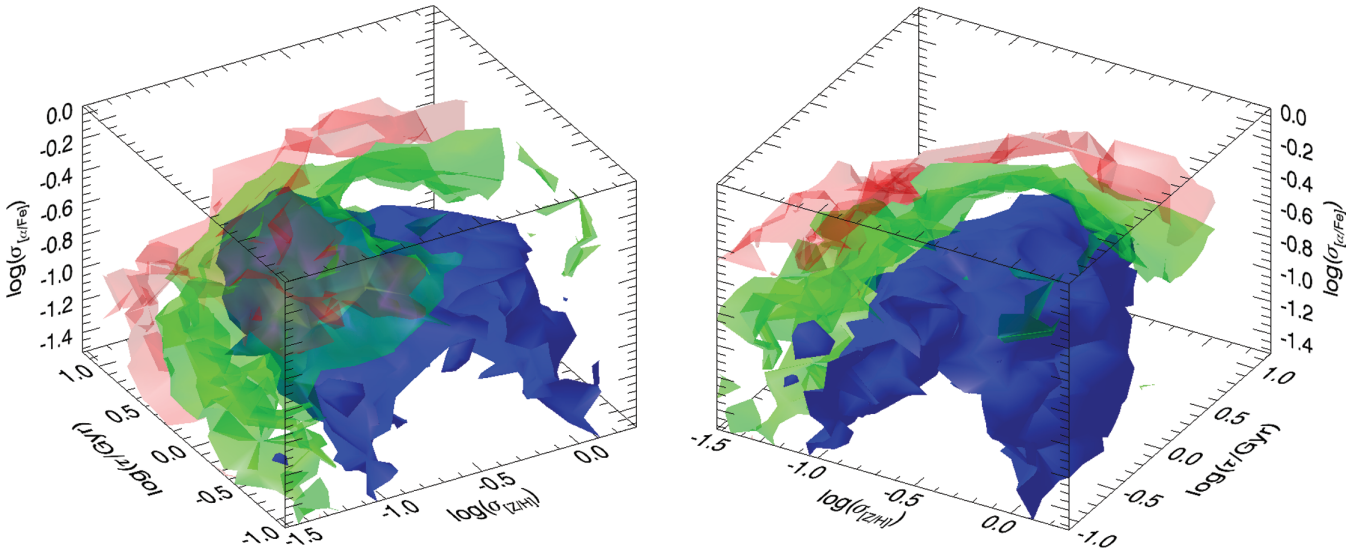

Figure 11. Two views of the 3D confidence contours of the e-folding of the exponential distribution of ages (τ) and the rms scatters in the Gaussian distributions of [Z/H] and [α/Fe] ($\sigma_{[Z/H]}$ and $\sigma_{[\alpha/Fe]}$), generated from the numerical simulations described in the text. The blue, green and red surfaces are the 1, 2 and 3σ confidence contours, respectively.

to line-strengths (and vice versa), it is not feasible to estimate SPPs using all available indices. Therefore, for this exercise, we rely on the three indices used earlier in investigating the anticorrelation between the age and [Z/H], that is, Hβ, Mg*b* and Fe5335.

With this combination of indices, galaxies in the cluster sample have an age distribution that is approximately exponential, and [Z/H] and [α/Fe] have distributions that are approximately Gaussian (see Fig. 5). Therefore, we began by selecting a range of e-foldings for the exponential age distribution (τ = 0.10, 0.15, 0.30, 0.55, 0.90, 1.60, 2.80, 5.00, 8.50, 15.00 Gyr), and ranges of Gaussian scatters in [Z/H] ($\sigma_{[Z/H]}$ = 0.03, 0.05, 0.08, 0.12, 0.20, 0.30, 0.50, 0.80, 1.25, 2.00 dex) and [α/Fe] ($\sigma_{[\alpha/Fe]}$ = 0.03, 0.04, 0.07, 0.10, 0.15, 0.20, 0.30, 0.45, 0.70, 1.00 dex). Each range was chosen to be approximately evenly spaced logarithmically so as to have better resolution at small values. The medians of the cluster [Z/H] and [α/Fe] distributions were used as the means of their Gaussian distributions, and the exponential age distribution was truncated at 5 Gyr (because the models are less reliable at young ages) and at 14 Gyr (the age of the Universe).

A model was generated for each combination of τ, $\sigma_{[Z/H]}$ and $\sigma_{[\alpha/Fe]}$, consisting of 10 000 mock galaxies with ages, [Z/H] and [α/Fe] (parameter triples) drawn randomly from the specified distributions. If any of the mock galaxies had a [Z/H] or [α/Fe] that fell outside the extent of the models,[1] then they were assigned the closest value from the models; this was not necessary for the ages since they were truncated at the values stated above.

These parameter triples were converted, via the Thomas et al. models, to the corresponding Hβ, Mg*b*and Fe5335 index values (index triples). This was achieved as follows. The models were divided into cells defined by two adjacent values of each SPP and for each mock galaxy the cell in which it fell was determined. Each cell is also defined by eight values of Hβ, Mg*b*and Fe5335, corresponding to their values at the eight vertices of the cubical cell. The index triple corresponding to the parameter triple is then calculated by taking the mean of each of these eight index values weighted by the distance in the parameter space of the mock galaxy from each corner of the cell.

These index triples were then perturbed by randomly drawing errors from an observed galaxy's index error distributions. In doing this, we cycled through the observed galaxies so that each observed galaxy had an approximately equal number of mock galaxies perturbed by its index error distributions. The perturbed index triples were converted back to parameter triples.

To ascertain how well the models fit the data, a likelihood statistic was used. The SPP space was divided into bins and the probability of each bin containing a galaxy was calculated. The age bins were 0.5 Gyr in width and ranged from 0 to 15 Gyr, the [Z/H] bins were 0.125 dex in width and ranged from −2.2875 to 0.7125 dex and the [α/Fe] bins were 0.025 dex in width and ranged from 0.0 to 0.5 dex. This resulted in 30 age bins, 24 [Z/H] bin and 20 [α/Fe] bins. Before the likelihood statistic was calculated, the model was lightly smoothed to minimize the number of bins with zero probabilities; a 3D Gaussian, with σ = 2/3 bins for all dimensions, was used as the smoothing kernel and bins within 3σ, in each dimension, were used in calculating the value of the bin probability in the smoothed model (i.e. two bins on either side in each dimension were used). The likelihood statistic is obtained by determining which bins the observed galaxies lie in and summing the logarithm of the bin probabilities.

Monte Carlo simulations were used to estimate the probability of obtaining a likelihood statistic larger than the observed one by chance. There are 103 galaxies with measurements of the indices required to estimate the SPPs in the cluster sample, so we simulate 103 galaxies in an identical manner to the model and calculate the maximum-likelihood statistic. This is done 10 000 times. The fraction of simulations with likelihood statistics larger than the observed value is recorded and 3D confidence contours are generated.

These 3D confidence contours are shown in Fig. 11, which presents the likelihood of our data set being represented by a model with the specified e-folding of the exponential distribution of ages and specified rms scatters in the Gaussian distributions of [Z/H] and [α/Fe]. While Fig. 11 provides an overall picture of the acceptable

[1] The Thomas et al. (2003) models have $1 \leq t \leq 15$ Gyr, $-2.25 \leq$ [Z/H] ≤ 0.67 dex and $0.0 \leq$ [α/Fe] ≤ 0.5 dex.

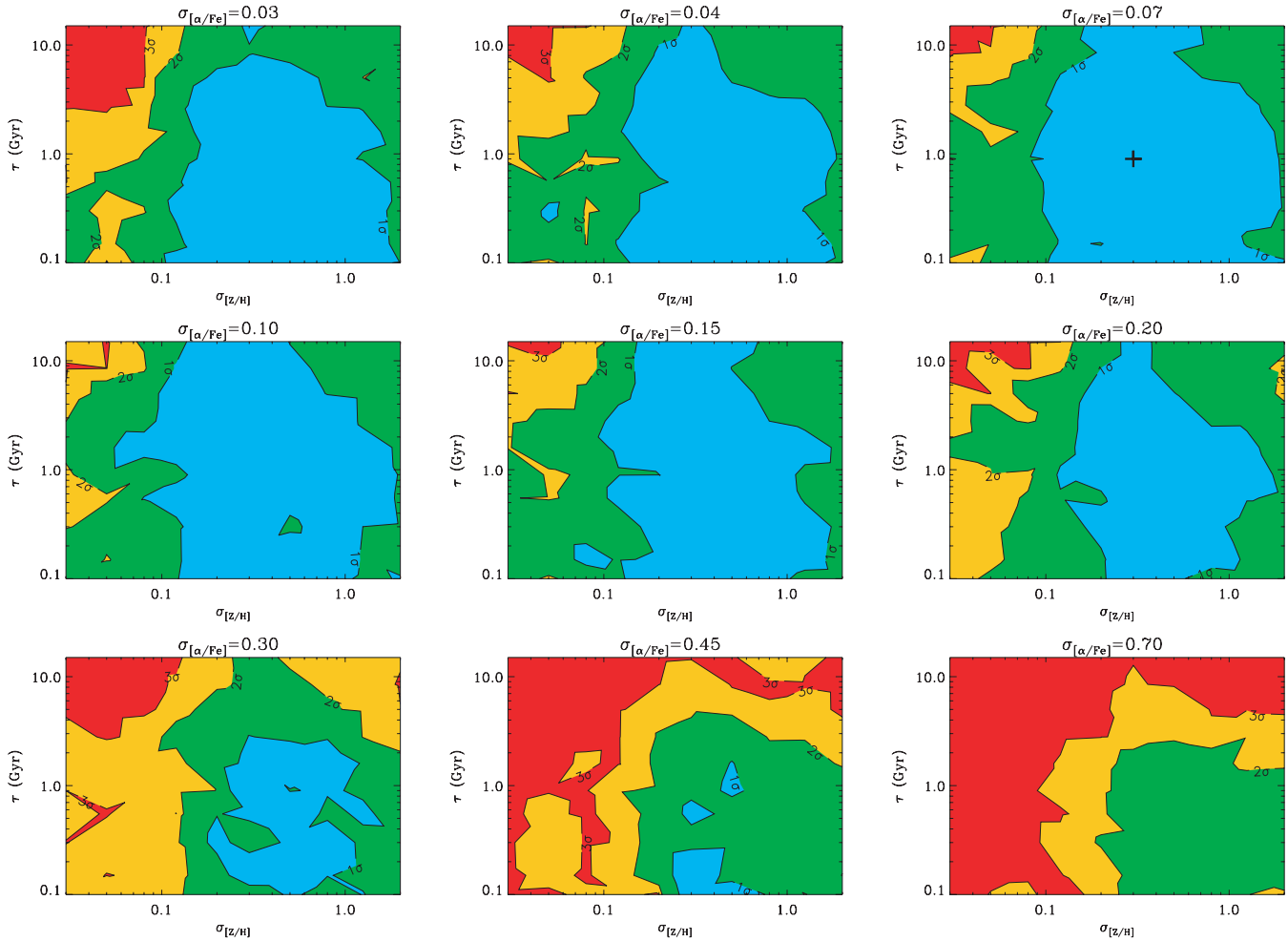

Figure 12. Slices, parallel to the age–[Z/H] plane, through the 3D confidence contours shown in Fig. 11. Blue is $<1\sigma$, green 1–2σ, orange 2–3σ and red $>3\sigma$. The value of the [α/Fe] scatter used to generate the model is shown at the top of each panel. The cross in the panel with [α/Fe] = 0.07 marks the model that is most consistent with our data.

scatters in the SPPs, more detailed information can be revealed by taking slices through the 3D confidence contours. Fig. 12 shows slices taken parallel to the age–[Z/H] plane at values of [α/Fe] corresponding to those used in generating the models.

These simulations provide us with a great deal of information regarding the intrinsic scatter in each of the SPPs. First, it is difficult to constrain the e-folding of the exponential age distribution. This is due to small uncertainties in line-strengths translating to large changes in the age estimate combined with relatively large observational errors in the Hβ index. Although models with small values of the e-folding are not ruled out, we find that our data are most consistent with the model having $\tau = 900$ Myr. Secondly, small scatters in [Z/H] ($\sigma_{[Z/H]} < 0.1$ dex) are strongly ruled out, as are large scatters ($\sigma_{[Z/H]} > 2.0$ dex). We find that the model with $\sigma_{[Z/H]} = 0.3$ dex is the most consistent with our data. Finally, large scatters in [α/Fe] ($\sigma_{[\alpha/Fe]} > 0.3$ dex) are also strongly ruled out. Models with low scatters in [α/Fe] are not ruled out, but we find that the most-consistent model is that with $\sigma_{[\alpha/Fe]} = 0.07$ dex. The model that gives the maximum likelihood (i.e. $\tau \sim 900$ Myr, $\sigma_{[Z/H]} \sim 0.3$ dex and $\sigma_{[\alpha/Fe]} = 0.07$ dex) is marked by a cross in Fig. 12.

Since the SPPs were found to be correlated with the velocity dispersion and since the galaxies in the cluster sample have a range of velocity dispersions, it is understandable that we should detect an intrinsic scatter in the SPP distributions. The degree to which the intrinsic scatter in the parameter distributions is attributable to trends with the velocity dispersion can be estimated by comparing the scatter expected, given the velocity dispersion distribution in the cluster and the intrinsic scatter about the parameter–σ relations.

We use the parameter–σ relations to convert the galaxies' velocity dispersions into parameter values. The scatter in these values is then calculated; the intrinsic scatter about the relation (as found in Section 5.1) is then added in quadrature to the scatter due to the relation with the velocity dispersion and the result is compared to that obtained from the simulations described above. We do this only for [Z/H] and [α/Fe], which were found to have approximately Gaussian distributions.

The scatter expected in [Z/H] on this basis is 0.21 dex which is comparable to the intrinsic scatter of $\sigma_{[Z/H]} \sim 0.3$ dex estimated above. The expected scatter in [α/Fe] is 0.06 dex which is very close to the estimated intrinsic scatter $\sigma_{[\alpha/Fe]} \sim 0.07$ dex. It appears then that the intrinsic scatter in both the [Z/H] and [α/Fe] distributions can almost entirely be accounted for by the parameter–σ relation and the intrinsic scatter about it.

For [Z/H], the scatter due to the correlation is 0.16 dex, while the intrinsic scatter about the relation is 0.13 dex; thus, most of the

intrinsic scatter in the [Z/H] distribution comes from the correlation with the velocity dispersion. For [α/Fe], the scatter due to the correlation is 0.03 dex, while the intrinsic scatter about the relation is 0.05 dex; thus, most of the intrinsic scatter in the [α/Fe] distribution comes from the intrinsic scatter about the [α/Fe]–σ relation.

7 DISCUSSION

The process by which galaxies form and the factors with the greatest influence on their evolution are unresolved issues. In models of the galaxy formation based on the hierarchical merging in a ΛCDM universe (e.g. De Lucia et al. 2006), the merger history of an early-type galaxy can fall anywhere between two extremes: mergers could occur early on and rapidly with the subsequent passive evolution – the revised monolithic collapse scenario (e.g. Merlin & Chiosi 2006); or the galaxy could experience a more prolonged history of mergers – the extended merging scenario (e.g. Toomre 1977). The environment of a galaxy and its mass are the two most influential factors on galaxy evolution but their effects need to be disentangled to gain an insight into the relative importance of each.

For cluster galaxies, the numerical simulations performed here show that the intrinsic scatters in [Z/H] and [α/Fe], and the e-folding of the exponential distribution of ages, are all quite small, as would be expected from a rapid formation at high redshift followed by passive evolution. Additionally, positive correlations are found between all three of the SPPs and velocity dispersion. The correlations found for both [Z/H] and [α/Fe] confirm well-known trends (Trager et al. 2000a; Kuntschner et al. 2001; Proctor & Sansom 2002; Thomas et al. 2002; Caldwell et al. 2003; Mehlert et al. 2003; Nelan et al. 2005; Thomas et al. 2005; Bernardi et al. 2006; Gallazzi et al. 2006; Kelson et al. 2006; Sánchez-Blázquez et al. 2006; Thomas et al. 2010). However, the correlation found for the age is not widely recognized; some authors find the age and velocity dispersion to be positively correlated (Proctor & Sansom 2002; Proctor et al. 2004a,b; Nelan et al. 2005; Thomas et al. 2005; Bernardi et al. 2006; Gallazzi et al. 2006; Thomas et al. 2010), while others find they are not correlated at all (Trager et al. 2000a; Kuntschner et al. 2001; Terlevich & Forbes 2002). Not only do we find that the age is positively correlated, but also that it is the most significantly correlated out of the three SPPs, being significant at the 5σ level. These correlations are qualitatively consistent with more recent semi-analytic models (De Lucia et al. 2006). These models incorporate feedback from active galactic nuclei (AGNs) (Croton et al. 2006), which heats the available gas, preventing further star formation in massive galaxies and bringing the predicted scaling relations into agreement with those observed.

There is a level of homogeneity to early-type cluster galaxies evidenced in the similarity of their line-strength and SPP distributions, and the consistency of the correlations between these quantities and velocity dispersion that is found between the clusters studied here. That this homogeneity is maintained amongst clusters of varying richness and morphology indicates that differences in the cluster environment have relatively little effect on the stellar populations of early-type galaxies. The dominant factor appears to be the mass.

While the mass plays a major role in determining the SPPs in early-type galaxies, it does not do so completely. The size of the role played varies; while [Z/H] is almost entirely a function of the velocity dispersion, [α/Fe] is less so. The intrinsic scatters in [Z/H] and [α/Fe] in the cluster galaxies were found to be almost entirely accounted for by the scatter produced by the correlations with the velocity dispersion and the intrinsic scatter about these relations.

Galaxies in low-density environments are observed to be, on average, $\sim$2 Gyr younger than galaxies in clusters (Trager et al. 2000a; Poggianti et al. 2001; Kuntschner et al. 2002; Terlevich & Forbes 2002; Caldwell et al. 2003; Proctor et al. 2004b; Denicoló et al. 2005; Thomas et al. 2005; Bernardi et al. 2006; Sánchez-Blázquez et al. 2006). The situation is not so clear with regards to differences in [Z/H] and [α/Fe]. Recent models predict that galaxies in denser environments are older and more metal rich than isolated galaxies (De Lucia et al. 2006). We do not find significant differences in the line-strength distributions or the SPP distributions between the cluster-outskirts sample and the cluster sample. However, the size of our SPP errors makes it difficult to detect the small differences in the age reported by other authors and any difference may be masked by the 1.3-Gyr offset to older ages found for galaxies that had their parameters estimated from fewer indices; such galaxies are found predominantly in the cluster-outskirts sample. We do find that the tight correlations with the velocity dispersion of both the line-strengths and SPPs that are found in clusters are weaker in the cluster outskirts, suggesting that the modes of formation in the cluster outskirts are more varied than those in the cluster cores.

Similar results were found by Thomas et al. (2010) who conclude that the formation and evolution of early-type galaxies are relatively insensitive to the environment and are instead driven by self-regulation processes and their intrinsic properties such as mass. However, our result that the SPP trends with the velocity dispersion are weaker in the cluster outskirts than in the clusters is in conflict with these results (see also Bernardi et al. 1998, 2006). The dip in ages found near the cluster virial radius (see Fig. 7) suggests that the movement into the cluster environment may induce a burst of star formation and, combined with the downsizing evident in Fig. 8, that this burst may occur preferentially in lower mass galaxies (similar to the rejuvenated population from Thomas et al.). Presumably, our two samples (cluster and cluster outskirts) are combined in their single high-density sample, which may result in the masking of this trend. Our results are broadly consistent with the results of Smith et al. (2006) who find a variation in the SPPs with the cluster radius. Thomas et al. find that the environment becomes more of an influence moving to less-massive galaxies (see also Haines et al. 2006).

Our results can be best explained by the revised monolithic collapse model, but is also consistent with the extended merging model if the mergers are dissipationless (see De Lucia et al. 2006). Pipino et al. (2009) have a model of the elliptical galaxy formation that implements a detailed treatment of the chemical evolution and they find that the correlation between [α/Fe] and the velocity dispersion is much less steep than that observed. Pipino et al. find that AGN quenching can help to improve the agreement, but this worsens their mass–metallicity relation compared to observations. They suggest that both relations can be reproduced, provided the formation of all spheroids happens quasi-monolithically, that is, the formation of the stars occurs in subunits and that this star formation and the assembly of the subunits into an elliptical galaxy occur at the same time and in the same place.

The star formation rates in galaxies are found to increase with increasing distance from the cluster centre and to converge to the mean field rate at distances greater than $\sim 3R_{\rm vir}$ times the virial radius (Lewis et al. 2002, see also Gómez et al. 2003). We find evidence that there is a dip in the mean ages of galaxies just inside the cluster virial radius, possibly due to the secondary star formation that reduces the luminosity-weighted mean age. This could be evidence that infalling galaxies, upon reaching the virial radius of a cluster, undergo a burst of star formation triggered by the dense intracluster medium.

If such a burst only amounted to a small fraction of the galaxy's total mass, then its effect on the integrated light would be short-lived and the galaxy would rapidly return to appearing old and red. Similar to the findings of Lewis et al., we find that this decrease in the age actually begins at $>3R_{\rm vir}$, suggesting that the influence of the cluster environment extends to large distances, whereas the result of Lewis et al. was based mainly on late-type galaxies; the remarkable thing about this result is that it applies to early-type galaxies.

There are two sources of bias that we must check have not influenced the above results: the number of indices used to derive the SPPs and the aperture corrections. It is possible that the lack of correlations with the velocity dispersion for the SPPs in the cluster-outskirts sample is due to the fact that, on average, fewer indices were used to estimate them than those in the cluster sample. This results in larger SPP errors and might potentially explain the lack of correlations with the velocity dispersion. However, as in Section 5.2, using only three indices to estimate the SPPs does not alter significantly their distributions compared to those derived from an unrestricted set of indices.

It is also possible that the mass segregation within the cluster could cause the weakening of the line-strengths in the cluster outskirts, if that is where less-massive galaxies are preferentially found. This is a result of the same aperture correction being applied to a galaxy, irrespective of how massive it is and despite the fact that the line-strengths being corrected were measured within differing effective radii. We find that our two samples (cluster and cluster outskirts) have a similar shape to their magnitude distributions, but that the galaxies in the cluster outskirts are on average $\sim$1 mag brighter, due to the facts that there are more galaxies in the cluster sample and that we target the brightest galaxies. So the correlation of weak line-strengths for less-massive galaxies cannot be the reason for the weakening of the trends with the velocity dispersion in the cluster-outskirts galaxies. We see no reason, therefore, in not believing that the weakening of the relations in the cluster outskirts is real.

The overall picture that emerges from this study is as follows. Early-type galaxies in clusters form a homogeneous class of objects that form in a process similar to a revised monolithic collapse and whose stellar populations are largely determined by their velocity dispersion (mass) and are relatively unaffected (at least differentially) by the cluster environment. The more massive they are, the older and more metal rich they become and the shorter their star formation time-scales are. The stellar populations of early-type galaxies in the outskirts of clusters, in contrast, appear less influenced by the mass, because, due to the varying environments they formed and evolved in, their evolutionary histories are more varied and this causes the correlations with the mass to be less significant. A galaxy, especially a less-massive one, that is falling into a cluster will, upon nearing the virial radius, undergo a burst of star formation. Once these stars have faded and ceased dominating the integrated light, the galaxy will appear indistinguishable from those in the cluster core.

8 SUMMARY

In summary, we have measured velocity dispersions, redshifts and absorption-line strengths for a magnitude-limited ($b_J \leqq 19.45$) sample of galaxies drawn from four clusters (Coma, A1139, A3558, and A930 at $\langle z \rangle = 0.04$) and their surrounds (extending to $\sim 10R_{\rm vir}$). Using the fully calibrated absorption-line indices coupled with the stellar population models of Thomas et al. (2003), we have estimated ages, [Z/H] and [α/Fe] for 219 galaxies. We have used these data to investigate the effects of the mass and environment on the stellar populations of early-type galaxies and our results can be summarized as follows.

(i) For galaxies in the cluster sample, all indices are positively correlated with the velocity dispersion, with the exceptions of H$\beta$and H$\beta_{\rm G}$, which are negatively correlated, and Fe5406, which is uncorrelated.

(ii) Only Mgb and H$\beta_{\rm G}$ are correlated with the velocity dispersion in the cluster-outskirts sample. The slopes of these two relations are consistent with those found for the cluster sample.

(iii) The cluster cores are relatively free from young galaxies and from galaxies that have experienced recent star formation. These galaxies are more commonly found outside $R_{\rm Abell}$.

(iv) The stellar populations in clusters form a homogeneous population. Despite the fact that our sample was drawn from four clusters spanning the ranges of BM classifications and Abell richness classes, the line-strength–σ relations, parameter–σ relations and SPP distributions are consistent between clusters.

(v) There is no difference between the line-strength distributions and SPP distributions in the clusters and their outskirts.

(vi) The SPPs in clusters are correlated with the velocity dispersion, suggesting that more massive galaxies are older, have shorter star formation time-scales and are more metal rich. These correlations are found to be weaker in the cluster outskirts.

(vii) For galaxies in the cluster sample, the e-folding time of the age distribution is 900 Myr, the intrinsic scatter in the [Z/H] distribution is 0.3 dex and the intrinsic scatter in the [α/Fe] distribution is 0.07 dex. The latter two intrinsic scatters can almost entirely be accounted for by the correlations with the velocity dispersion and the scatter about the relations. We conclude therefore that the mass of a galaxy plays a major role in determining its stellar populations.

Further high-quality observations of galaxies at higher redshifts will allow the development of a consistent model of the early-type galaxy formation at all masses and in all environments.

ACKNOWLEDGMENT

The authors thank the anonymous referee for a careful reading of this paper and for the many helpful suggestions that improved it considerably.

REFERENCES

Arimoto N., Yoshii Y., 1987, A&A, 173, 23
Balogh M. L., Schade D., Morris S. L., Yee H. K. C., Carlberg R. G., Ellingson E., 1998, ApJ, 504, L75
Bekki K., 1999, ApJ, 510, L15
Bender R., Burstein D., Faber S. M., 1993, ApJ, 411, 153
Bernardi M., Renzini A., da Costa L. N., Wegner G., Alonso M. V., Pellegrini P. S., Rité C., Willmer C. N. A., 1998, ApJ, 508, L143
Bernardi M. et al., 2003, AJ, 125, 1882
Bernardi M., Sheth R. K., Nichol R. C., Schneider D. P., Brinkmann J., 2005, AJ, 129, 61
Bernardi M., Nichol R. C., Sheth R. K., Miller C. J., Brinkmann J., 2006, AJ, 131, 1288
Blanton M. R., Eisenstein D., Hogg D. W., Schlegel D. J., Brinkmann J., 2005, ApJ, 629, 143
Boselli A., Gavazzi G., 2006, PASP, 118, 517
Bressan A., Chiosi C., Fagotto F., 1994, ApJS, 94, 63
Burstein D., Faber S. M., Gaskell C. M., Krumm N., 1984, ApJ, 287, 586
Burstein D., Faber S. M., Gonzalez J. J., 1986, AJ, 91, 1130
Burstein D., Davies R. L., Dressler A., Faber S. M., Lynden Bell D., 1988, in Kron R. G., Renzini A., eds, Proc. of the 5th Workshop of the Adv. Sch.

of Astron. Vol. 141, Towards Understanding Galaxies at Large Redshift. Kluwer, Dordrecht, p. 17
Caldwell N., Rose J. A., Concannon K. D., 2003, AJ, 125, 2891
Cardiel N., Gorgas J., Cenarro J., Gonzalez J. J., 1998, A&AS, 127, 597
Clemens M. S., Bressan A., Nikolic B., Alexander P., Annibali F., Rampazzo R., 2006, MNRAS, 370, 702
Colless M., Burstein D., Davies R. L., McMahan R. K., Saglia R. P., Wegner G., 1999, MNRAS, 303, 813
Colless M. et al., 2001, MNRAS, 328, 1039
Collobert M., Sarzi M., Davies R. L., Kuntschner H., Colless M., 2006, MNRAS, 370, 1213
Couch W. J., Sharples R. M., 1987, MNRAS, 229, 423
Cowie L. L., Songaila A., Hu E. M., Cohen J. G., 1996, AJ, 112, 839
Croton D. J. et al., 2006, MNRAS, 365, 11
Davies R. L., Sadler E. M., Peletier R. F., 1993, MNRAS, 262, 650
Davis M., Geller M. J., 1976, ApJ, 208, 13
De Lucia G., Springel V., White S. D. M., Croton D., Kauffmann G., 2006, MNRAS, 366, 499
Denicoló G., Terlevich R., Terlevich E., Forbes D. A., Terlevich A., 2005, MNRAS, 358, 813
Dressler A., 1980, ApJ, 236, 351
Eggen O. J., Lynden Bell D., Sandage A. R., 1962, ApJ, 136, 748
Faber S. M., Friel E. D., Burstein D., Gaskell C. M., 1985, ApJS, 57, 711
Fisher D., Franx M., Illingworth G., 1995, ApJ, 448, 119
Fisher D., Franx M., Illingworth G., 1996, ApJ, 459, 110
Gallazzi A., Charlot S., Brinchmann J., White S. D. M., 2006, MNRAS, 370, 1106
Gómez P. L. et al., 2003, ApJ, 584, 210
González J. J., 1993, PhD Thesis, University of California, Santa Cruz
Gorgas J., Faber S. M., Burstein D., Gonzalez J. J., Courteau S., Prosser C., 1993, ApJS, 86, 153
Graves G. J., Faber S. M., Schiavon R. P., Yan R., 2007, ApJ, 671, 243
Greggio L., 1997, MNRAS, 285, 151
Gunn J. E., Gott J. R. I., 1972, ApJ, 176, 1
Haines C. P., La Barbera F., Mercurio A., Merluzzi P., Busarello G., 2006, ApJ, 647, L21
Harrison C. D., Colless M., Kuntschner H., Couch W. J., De Propis R., Pracy M. B., 2010, MNRAS, 409, 1455
Hashimoto Y., Oemler A. J., 1999, ApJ, 510, 609
Jones D. H. et al., 2004, MNRAS, 355, 747
Jørgensen I., 1997, MNRAS, 288, 161
Jørgensen I., 1999, MNRAS, 306, 607
Jørgensen I., Franx M., Kjærgaard P., 1996, MNRAS, 280, 167
Kauffmann G., 1996, MNRAS, 281, 487
Kauffmann G., Charlot S., 1998, MNRAS, 294, 705
Kauffmann G., White S. D. M., Heckman T. M., Ménard B., Brinchmann J., Charlot S., Tremonti C., Brinkmann J., 2004, MNRAS, 353, 713
Kelson D. D., Illingworth G. D., Franx M., van Dokkum P. G., 2006, ApJ, 653, 159
Koeppen J., Weidner C., Kroupa P., 2007, MNRAS, 375, 673
Kuntschner H., 2000, MNRAS, 315, 184
Kuntschner H., Lucey J. R., Smith R. J., Hudson M. J., Davies R. L., 2001, MNRAS, 323, 615
Kuntschner H., Smith R. J., Colless M., Davies R. L., Kaldare R., Vazdekis A., 2002, MNRAS, 337, 172
Larson R. B., 1974, MNRAS, 166, 585
Larson R. B., 1975, MNRAS, 173, 671
Larson R. B., Tinsley B. M., Caldwell C. N., 1980, ApJ, 237, 692
Lewis I. et al., 2002, MNRAS, 334, 673
Mastropietro C., Moore B., Mayer L., Debattista V. P., Piffaretti R., Stadel J., 2005, MNRAS, 364, 607
Matković A., Guzmán R., Sánchez-Blázquez P., Gorgas J., Cardiel N., Gruel N., 2009, ApJ, 691, 1862
Mehlert D., Thomas D., Saglia R. P., Bender R., Wegner G., 2003, A&A, 407, 423
Merlin E., Chiosi C., 2006, A&A, 457, 437
Moore B., Lake G., Quinn T., Stadel J., 1999, MNRAS, 304, 465
Nelan J. E., Smith R. J., Hudson M. J., Wegner G. A., Lucey J. R., Moore S. A. W., Quinney S. J., Suntzeff N. B., 2005, ApJ, 632, 137
Norberg P. et al., 2002, MNRAS, 332, 827
Ogando R. L. C., Maia M. A. G., Pellegrini P. S., da Costa L. N., 2008, AJ, 135, 2424
Pipino A., Devriendt J. E. G., Thomas D., Silk J., Kaviraj S., 2009, A&A, 505, 1075
Poggianti B. M. et al., 2001, ApJ, 563, 118
Postman M., Geller M. J., 1984, ApJ, 281, 95
Press W. H., Teukolsky S. A., Vetterling W. T., Flannery B. P., 1992, Numerical Recipes in FORTRAN. The Art of Scientific Computing. Cambridge Univ. Press, Cambridge
Proctor R. N., Sansom A. E., 2002, MNRAS, 333, 517
Proctor R. N., Forbes D. A., Hau G. K. T., Beasley M. A., De Silva G. M., Contreras R., Terlevich A. I., 2004a, MNRAS, 349, 1381
Proctor R. N., Forbes D. A., Beasley M. A., 2004b, MNRAS, 355, 1327
Romeo A. D., Portinari L., Sommer-Larsen J., 2005, MNRAS, 361, 983
Sánchez-Blázquez P., Gorgas J., Cardiel N., González J. J., 2006, A&A, 457, 787
Sarzi M. et al., 2006, MNRAS, 366, 1151
Schindler S. et al., 2005, A&A, 435, L25
Searle L., Zinn R., 1978, ApJ, 225, 357
Smith R. J., Hudson M. J., Lucey J. R., Nelan J. E., Wegner G. A., 2006, MNRAS, 369, 1419
Smith R. J., Lucey J. R., Hudson M. J., 2007, MNRAS, 381, 1035
Terlevich A. I., Forbes D. A., 2002, MNRAS, 330, 547
Thomas D., Maraston C., Bender R., 2002, Ap&SS, 281, 371
Thomas D., Maraston C., Bender R., 2003, MNRAS, 339, 897
Thomas D., Maraston C., Korn A., 2004, MNRAS, 351, L19
Thomas D., Maraston C., Bender R., Mendes de Oliveira C., 2005, ApJ, 621, 673
Thomas D., Maraston C., Schawinski K., Sarzi M., Silk J., 2010, MNRAS, 404, 1775
Tinsley B. M., Gunn J. E., 1976, ApJ, 203, 52
Toomre A., 1977, in Tinsley B. M., Larson R. B., eds, Proceedings of a Conference at Yale University, Evolution of Galaxies and Stellar Populations. Yale University Observatory, New Haven, p. 401
Trager S. C., Worthey G., Faber S. M., Burstein D., Gonzalez J. J., 1998, ApJS, 116, 1
Trager S. C., Faber S. M., Worthey G., González J. J., 2000a, AJ, 120, 165
Trager S. C., Faber S. M., Worthey G., González J. J., 2000b, AJ, 119, 1645
Treu T., Stiavelli M., Bertin G., Carollo M., Casertano S., Möller P., 1999, BAAS, 31, 826
Treu T., Stiavelli M., Bertin G., Casertano S., Möller P., 2001, MNRAS, 326, 237
Treu T., Stiavelli M., Casertano S., Möller P., Bertin G., 2002, ApJ, 564, L13
Treu T., Ellis R. S., Liao T. X., van Dokkum P. G., 2005a, ApJ, 622, L5
Treu T. et al., 2005b, ApJ, 633, 174
van der Wel A., Franx M., van Dokkum P. G., Rix H.-W., 2004, ApJ, 601, L5
van der Wel A., Franx M., van Dokkum P. G., Rix H.-W., Illingworth G. D., Rosati P., 2005, ApJ, 631, 145
van Dokkum P. G., Stanford S. A., 2003, ApJ, 585, 78
van Dokkum P. G., Franx M., Kelson D. D., Illingworth G. D., 2001, ApJ, 553, L39
White S. D. M., Rees M. J., 1978, MNRAS, 183, 341
Worthey G., 1994, ApJS, 95, 107
Worthey G., Collobert M., 2003, ApJ, 586, 17
Worthey G., Ottaviani D. L., 1997, ApJS, 111, 377
Worthey G., Faber S. M., Gonzalez J. J., 1992, ApJ, 398, 69
Worthey G., Faber S. M., Gonzalez J. J., Burstein D., 1994, ApJS, 94, 687
Ziegler B. L., Bender R., 1997, MNRAS, 291, 527

This paper has been typeset from a TEX/LATEX file prepared by the author.